UNLV University Libraries
University of Nevada, Las Vegas

UNLV Theses, Dissertations, Professional Papers, and Capstones

8-2010

Field measurement & verification of residential duct leakage methods and CFD analysis of HVAC mixing box

Uday Vadlamani
University of Nevada, Las Vegas

Follow this and additional works at: https://digitalscholarship.unlv.edu/thesesdissertations

 Part of the Mechanical Engineering Commons

Repository Citation

Vadlamani, Uday, "Field measurement & verification of residential duct leakage methods and CFD analysis of HVAC mixing box" (2010). *UNLV Theses, Dissertations, Professional Papers, and Capstones*. 896.
https://digitalscholarship.unlv.edu/thesesdissertations/896

This Thesis is protected by copyright and/or related rights. It has been brought to you by Digital Scholarship@UNLV with permission from the rights-holder(s). You are free to use this Thesis in any way that is permitted by the copyright and related rights legislation that applies to your use. For other uses you need to obtain permission from the rights-holder(s) directly, unless additional rights are indicated by a Creative Commons license in the record and/or on the work itself.

This Thesis has been accepted for inclusion in UNLV Theses, Dissertations, Professional Papers, and Capstones by an authorized administrator of Digital Scholarship@UNLV. For more information, please contact digitalscholarship@unlv.edu.

FIELD MEASUREMENT & VERIFICATION OF RESIDENTIAL DUCT LEAKAGE METHODS AND CFD ANALYSIS OF HVAC MIXING BOX

by

Uday Vadlamani

Bachelor of Technology in Mechanical Engineering
Jawaharlal Nehru Technological University, India
May 2007

A thesis submitted in partial fulfillment
of the requirements for the

Master of Science Degree in Mechanical Engineering
Department of Mechanical Engineering
Howard R. Hughes College of Engineering

Graduate College
University of Nevada, Las Vegas
May 2010

Copyright by Uday Vadlamani 2010
All Rights Reserved

UNLV
UNIVERSITY OF NEVADA LAS VEGAS

THE GRADUATE COLLEGE

We recommend that the thesis prepared under our supervision by

Uday Vadlamani

entitled

Field Measurement & Verification of Residential Duct Leakage Methods and CFD Analysis of HVAC Mixing Box

be accepted in partial fulfillment of the requirements for the degree of

Master of Science in Mechanical Engineering

Samir F. Moujaes, Committee Chair

Robert F. Boehm, Committee Member

Woosoon Yim, Committee Member

Moses Karakouzian, Graduate Faculty Representative

Ronald Smith, Ph. D., Vice President for Research and Graduate Studies and Dean of the Graduate College

August 2010

ABSTRACT

Field Measurement & Verification of Residential Duct Leakage Methods and CFD Analysis of HVAC Mixing Box

by

Uday Vadlamani

Samir F Moujaes, Ph.D., P.E., Examination Committee Chair
Professor, Department of Mechanical Engineering
University of Nevada, Las Vegas

The research work in this thesis is subdivided to providing the initial results of the experimental work followed by simulation work at the end. The experimental work proposes a new measurement technique for measuring total and local leakages in ducts. The experimental work in this research tries to focus effort on finding the approximate locations of leaks in the HVAC residential duct systems to direct better the effort of duct sealing. This technique can provide several advantages over existing techniques. It will eventually have a greater potential to locate leaks so that retrofitting in ducts can be focused on leaky locations. Field studies were performed in 11 houses in Las Vegas. Out of these, 4 houses were selected for fixing the leakages in them and the tests were repeated on these houses to verify the duct leakage reduction and benefits. The proposed method can offer a more cost effective approach when compared to other methods in the future. It reduces the total

leakage for different houses by 14.4% to 46.5% of the total initial leakage rate.

The second part of this thesis consists of performing a 3-D, k-ε turbulent CFD study of HVAC Mixing box. Return air is supplied from the top of the box and outside air supplied from the back of mixing box. The temperature and velocity profiles of air in the HVAC mixing box were analyzed. The effects of carbon dioxide concentration in the mixing box were also analyzed. The current CFD simulation results were compared to previous field measurements of temperature stratification in a mixing box published in the International Journal of Energy Research in 2001. The CFD results showed that within the experimental error given in the previous paper the CFD temperature distribution predictions were reasonably close to the experimental results indicating that a detailed CFD approach can be used for predictive purposes.

ACKNOWLEDGEMENTS

I would like to take this opportunity to express my gratitude to those who have helped me bring this thesis to a successful end with their knowledge, help and co-operation.

I would like to thank Dr. Samir Moujaes, my research advisor for all the support and guidance he has offered me during the course of my graduate studies at University of Nevada, Las Vegas. His encouragement and valuable suggestions have helped me immensely in seeking the right direction for this thesis. I would like to thank my committee member, Dr. Robert Boehm for his patience and effort in reviewing my thesis. I am grateful to Dr. Woosoon Yim for being in my committee. I would also like to thank Dr.Moses Karakouzian who has accepted to be my graduate college representative.

This thesis has been a challenging experience to me and was accomplished through the help of many people. In particular, I extend my appreciation and thanks to graduate students, Sucharita Akula and Nagurbabu for their help during the model development and analysis. I thank the Department of Mechanical Engineering, UNLV, for providing me financial support throughout the coursework and for providing timely support and infrastructure to finish my thesis.

My deepest gratitude to my parents Seshagiri Rao Vadlamani and Kamala Vadlamani for their love, care and opportunities they have provided me at every stage of my life. I shall remain ever obliged to my uncle, Vishanatham Peri and all my cousins for their continuous support in all my endeavors. Last but not the least, I would like to thank all my friends and roommates for their support.

TABLE OF CONTENTS

LIST OF FIGURES

LIST OF TABLES

CHAPTER 1

LITERATURE REVIEW

Duct leakage in forced-air distribution systems has a significant impact on the energy consumed in residential buildings [1] [2]. Field studies have shown that existing residential systems can lose up to 40% of the total supply air in the form of duct leakage [3]. As ducts are often outside the conditioned space, this leakage corresponds to a proportionate amount of energy loss from the duct system which would have rather been used to heat or cool the conditioned space [4]. There is also humidity, comfort, and indoor air quality problems associated with return duct leaks drawing air from outside or unconditioned spaces within the structure [5][6][7].

In addition, a system with more return than supply leakage causes increased infiltration which must be conditioned [4].Several methods for estimating duct leakage have been used in the past with varying degrees of accuracy. One of the widely used techniques is the duct pressurization test that is part of ANSI/ASHRAE Standard 152-2004 [8].

The leakage, in this test, is estimated by measuring the flow from a calibrated fan into the duct system at usually one test pressure (e.g. 25 Pa). The blower door can be used simultaneously to pressurize the house to measure the leakage to outside. More recently, Delta Q and Nulling tests have been used to find total duct leakage. The Delta Q [9] [10] [11]

[12] uses the difference in blower doors at each of several pressure stations to estimate duct leakage. The Nulling test [13] [14] [15] uses a calibrated fan to counteract the pressure change across the envelope due to duct leakage.

All of these techniques focused on determining the total supply and return leakages irrespective of where the leaks are located along the air ducts. These leakage rate tests are determined at an average pressure not necessarily at the values of local pressure at which a particular local leakage process is taking place. It is generally accepted that a particular leakage rate is proportional to the pressure difference across it with all other parameters being equal. The location and the nature of the leak may be particularly important in selecting the methods to mitigate some of these leaks more cost effectively than what is available now. Therefore, a technique for estimating the "local" and "total" leakage may be a cost effective way to target resources on leaky homes and to focus efforts on portions of ducts that have the worst problems. This thesis proposes a new measurement technique for estimating the local and total leakage rates. The technique can provide several advantages over existing measurement techniques. It has a potential to locate leaks so that retrofitting in ducts can be focused on leaky locations. It can also estimate the total leakage more accurately to focus the repair jobs on the right houses.

CHAPTER 2

INTRODUCTION

Field tests have been performed in 11 residential houses in the Las Vegas area to validate the laboratory results. A field study has been done on these houses in which the tests can be repeated and then the improvement on the test protocol or equipment used can be made. Different techniques for measuring air duct leakages, including duct pressurization, zone bag tests, and Delta Q, have been investigated. A subset of these 11 houses was then chosen and the leakages in these houses are fixed by using standard means of duct sealing techniques using a local contractor. The houses which are fixed are retested to determine the potential reduction of duct leakage.

The main objectives of this field study research are:

- To investigate the component sources of typical residential air duct leakages through the development of potentially new technologies.
- To assess cost effective ways to seal air duct leaks depending on the percentage of total leak and location of the leaks in the residential duct system.

These objectives were achieved by incorporating the following steps

- Establishing an experimental facility Air Duct Leakage Laboratory (ADLL).

- Performing field testing for potential leakages in 11 houses in Las Vegas.
- Fixing the leakages in houses with the help of a local HVAC contractor and retesting the houses.
- Doing cost analysis and calculating the payback period.

The key contributions of this research are:

- Identification of leak locations and precise quantitative estimation of local and total leakage rates using a new experimental technique on the local houses in Las Vegas.
- Fixing the duct leakages in houses.
- Providing cost effective methods to fix duct leakages in houses.

2.1 Instrumentation

The instruments used for the laboratory and field testing are discussed in this chapter. The equipment is purchased from Energy Conservatory.

2.1.1 Zone Bag

Zone bags are made up of a thick inner bladder covered with a layer of puncture resistant vinyl cloth and the open end of the rubber bladder is connected to a PVC hose through which the bag can be pressurized as shown in Figure 1. The hose has a ball valve on its end. The zone bags are introduced into a section of the duct and then inflated using compressed air by connecting the ball valve to a compressor. In a

completely inflated state the zone bag fills into the ridges of the helical groves of the flex duct to give a larger area of contact to provide air tightness. Zone bags can be introduced into the duct to isolate the air flow sequentially from the air outlet supplies upstream to the fan. This allows sequential determination of where leaks exist and to what percentages they do exist as part of the overall duct leakage. Zone bags are generally used in duct cleaning to block sections of ducting to make major jobs more manageable.

Figure 1. Zone bag with nominal diameter of eight inches

2.1.2 Duct Blaster

The duct blaster is a calibrated air flow measurement system designed to test the air tightness of forced air duct systems (Figure 2). The air flow

through the duct blaster fan required to pressurize the duct system to the test pressure is the measured total duct leakage rate at that operating pressure.

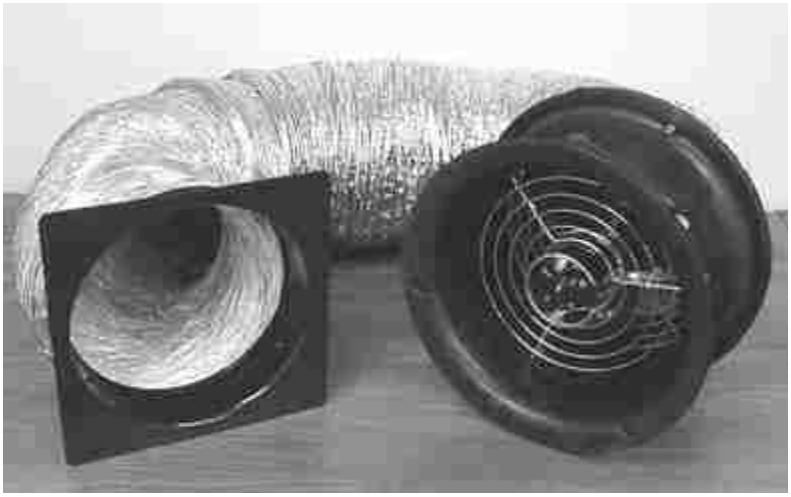

Figure 2. Duct Blaster

The duct blaster fan consists of molded fan housing with a variable speed motor. The duct blaster fan can move up to 1,500 cubic feet of air per minute (cfm) at zero back pressure (i.e. free air), and approximately 1,350 cfm against 50 Pa of back pressure. With the flexible extension duct attached, the fan can move 1,250 cfm (free air) and 1,000 cfm against 50 Pa of back pressure. Fan flow is determined by measuring the slight vacuum created by the air flowing over the flow sensor attached to the end of the motor. The duct blaster fan can accurately measure flows between 10 and 1,500 CFM using a series of three calibrated flow rings

which are attached to the fan inlet. Though the duct blaster fan motor is not reversible, the fan can be installed to either pressurize or depressurize the duct system.

2.1.3 Blower Door

The blower door is a calibrated fan used to measure building air tightness. It is fixed into an exterior doorway. The fan blows air into or out of the building to create a pressure difference between inside and outside. The pressure difference forces air through all holes and penetrations in the exterior envelope. By measuring the air flow through the fan and its effect on the air pressure in the building, the blower door system measures the air tightness of the building envelope.

Figure 3. Typical blower door setup

The kit consists of the fan, the fan speed controller and the adjustable aluminum door frame. The blower door fan can accurately measure airflow over a wide range of flow rates using a series of calibrated flow rings which are attached to the inlet of the fan. Figure 3 shows the blower door in a typical building diagnostics setup.

2.1.4 DG 700 Pressure and Flow Gauge

The DG-700 pressure and flow gauge manufactured by Energy Conservatory is a multi-functional differential pressure gauge with two independent measurement channels.

Figure 4. Pressure and flow gauge made by Energy Conservatory

In addition to providing high resolution pressure measurements, the DG-700 is programmed to provide air flow measurements during

building performance test procedures based on the information about the type of calibrated fan and the flow ring. Figure 4 shows the DG 700 pressure gauge.

2.1.5 Register Sealing Film

Register sealing film is an adhesive backed plastic that can be used to provide a quick temporary seal on registers (Figure 5) when measuring duct leakage with a duct blaster or blower door. It is made by The Energy Conservatory. The film can be easily removed from the register and does not harm the register's finish. It is available in 8" and 24" width rolls. It is perforated at regular lengths to provide easy dispensing.

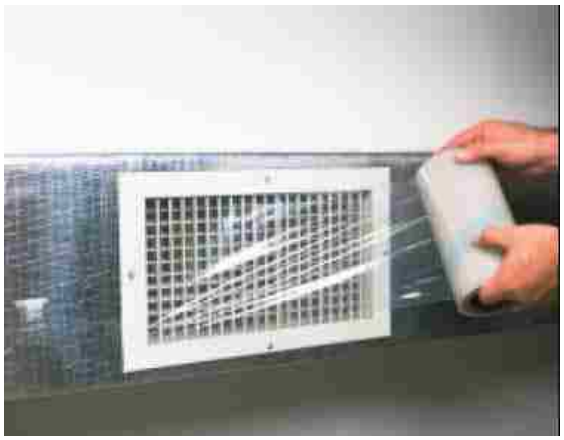

Figure 5. Register sealing film by conservation strategies [16]

2.1.6 Visual Inspection System

The visual inspection system is an inspection tool for air conditioning systems (Figure 6). This tool was used to confirm the leak location

information obtained by local leak detection techniques. It consists of a high resolution color camera head consisting of six LEDs with diffusers and 25-foot reinforced vinyl insertion cable. The camera can be connected to a laptop or a television screen using appropriate cables to view the inside of the duct in real time.

Figure 6. Visual Inspection System

2.1.7 Pressure Pan

The pressure pan is a quick diagnostic tool for leak detection. It is a shallow pan with a pressure tap in the middle and rubber gasketed edges.

Figure 7. Pressure pan by conservation strategies [17]

For testing, the blower door is used to pressurize or depressurize the house to a test pressure. The pressure pan is placed over each of the registers and the pressure difference across each register is measured, as shown in Figure 7. A large pressure difference indicates that the leak is nearer to the register. Pressure pans are available in two sizes: 12"x14"x4" and 22"x22"x2".

CHAPTER 3

FIELD TESTING

3.1 Field Test Preparation

The main objective of this project is to validate the laboratory results of the test in the field using several homes in the Las Vegas area. It is desired to apply this new technique to quantify the duct air leakage rates from several sections of a typical duct subjected to various levels of pressure differences between the ambient duct air and the environment outside that duct. However, the objective of the "field test preparation" is to select the house that is suitable for testing, tune and identify the test protocols of the techniques tested, and train the team members by conducting initial tests on 11 real houses.

3.2 Survey and Selection of Residential Field Test Buildings

A detailed information list of each potential house to be selected was filled which includes all the necessary spatial and system information regarding that house. This short survey is needed as part of the overall record keeping. The two parameters that the research group focuses on for the selection are the age and the size of the buildings with emphasis on ducts in the attic. As regards to age of the home the choice was made to use some older buildings (pre 1990) and some newer ones. In regards to the size, a range of layouts was chosen between 1,500 to 3,400 sq. ft.

of living space is selected for that purpose as it represents the most likely size range of a typical home in the Las Vegas area. It is expected that methods of construction of newer buildings have improved over the years such that newer homes are expected to be less leaky than older ones. Also the methods of installation and materials used in flexible ducts and their sealants have improved over the years as well. Finally the age of the home could present a variation of ceiling height between old and newer buildings. The home size being considered as a parameter will affect the capacity of the HVAC units, hence the supply flow rates, the duct surface area which introduces the possibility of more duct leaks due to the potential of having more duct fittings and more registers.

Based on the criteria mentioned above (living space of home) and on the additional baseline duct leakage test described in ASHRAE 152-2004 the final selection of the buildings is made. An additional criterion for the house selection was the percentage of duct leakage flow as compared to the total supply flow rate under which a building would not be selected i.e. less than 10% of total air handling flow rate. Hence the final choice includes a total of eleven buildings. Within this very limited population other factors will also be noted such as duct insulation, number of supply and return registers, building volume, presence of radiant barriers if any, reduced-absorptivity coatings and tile roofs.

3.3 Test Protocol

The test procedure of the proposed technique used for field test combines two main sets of tests: (i) screening test and (ii) zone bag tests [18].

The following test procedure shall be used for the screening test (total leakage estimation):

1) Block the supply from the return at either the supply or return plenum. System air filters are often located in an ideal location for this blockage and can be replaced with blocking materials.

2) Seal off all supply and return registers

3) Install the calibrated fan (flow meter) at air handler cabinet to pressurize either the supply side or return side

4) Install pressure probes at the supply and return plenums to record the pressure difference between supply/or return duct and the house (ΔPs_H and ΔPr_H). Alternative locations such as the nearest registers may be used for pressure measurement instead. In addition, it is required to measure the pressure difference (ΔPs_{L1}) in one selected location far from supply plenum (close to the end of supply duct) which will be used for accurate local leakage estimation in the zone bag tests.

5) Adjust the calibrated fan to provide 25 Pa measured at the supply plenum (ΔPs_H) when the supply side is being pressurized, or to measure the return plenum (ΔPr_H) pressure at 25Pa when the return side is being pressurized.

6) Record the flow through the flow meter Q_{f1} as an indication of total supply or return leakage.

The following procedure shall be used for zone bag (ZB) tests (local leakage estimation):

1) Select one accessible register, preferably in the middle of the supply duct. Insert the ZB through the opened register to be located in the main supply duct. The duct will then be broken into two main sections H (upstream of ZB) and L (downstream of ZB).

2) Cover the opening of the removed register by a designed cover assembled with the ZB. This cover is equipped with a pressure probe to measure the pressure inside the duct. It is assumed that the measured supply plenum pressure difference (ΔPs_H) represents the leak pressure in the entire section H and the pressure difference measured by the probe installed at the ZB cover represents the leak pressure in the entire section L(ΔPs_L).

3) Inflate the ZB using compressed air and monitor the pressure (ΔPs_L) at the pressure pan of the ZB assembly. Stop inflating the zone bag when the pressure difference ΔPs_L becomes less than 5 Pa.

4) Readjust the flow meter to maintain the original supply plenum difference (ΔPs_L) (i.e., 25 Pa)

5) Record the new flow through the calibrated fan Q_{f2} and the new pressure difference in section L (ΔPs_{L2}).

6) Calculate the flow difference ΔQ ($Q_{f,2}$-$Q_{f,1}$) and the correction factor CF by the following equation: $CF = \frac{1}{1-\left(\frac{\Delta Ps_{L2}}{\Delta Ps_{L1}}\right)^n}$

7) Determine the leakage in section L (Qs_L) as the product of the flow difference ΔQ_f and correction factor CF. Determine also the leakage in section H (Qs_H) by subtracting the leakage in section L from the total supply leakage Q_{f1}.

The steps 1 to 7 are repeated to cover other duct sections branching out from the supply plenum.

3.4 Initial Field Test

A field study was made on 11 real houses in which the tests can be repeated and then improvement on the test protocol or equipment used can be made. Different leakage techniques including the proposed technique were applied to some of the homes. The techniques with the required equipment are listed in Table 1. The techniques tested are duct pressurization test, zone bag technique (proposed technique), subtraction technique, pressure pan, and Delta Q. The eventual aim of using the developed technique was to provide a minimum time required to complete that test. The sequence of the tests is as follows:

1. Duct pressurization test: All registers are sealed off and the duct blaster is installed.

2. Zone bag tests: One register located in the middle of the duct is opened the zone bag is inserted and inflated inside the duct to create an artificial restriction. The zone bag tests are repeated to cover the required registers

3. Duct pressurization test (leakage to outside): The blower door is installed and then the tests with both duct blaster and the blower door are performed as described in ASHRAE Standard

4. Subtraction technique: The duct blaster is removed and the house is depressurized and pressurized to multiple pressures by the blower door while the registers are still sealed off. The tests are repeated while the registers are no longer sealed. This test was not performed on the houses due to time constraints.

5. Pressure pan technique: During the house depressurization mode (-50 Pa) and while the registers are no sealed, the pressure pan covered one register each time and the pressure was recorded.

6. Delta Q technique: The house is again depressurized and pressurized to multiple pressures while the air handler is turned on.

The operating pressures are measured using the pressure pan and pressure probe. The total flow of the air handler fan is measured by using the True Flow meter. Based on the requirement for time to complete each test and due to the time constraints, only some of the above techniques are applied to the houses.

Table 1. Techniques considered in field tests

Techniques considered in field testing	**Equipment required**
Duct pressurization test (total)	Duct blaster
Duct pressurization test (Leakage to outside)	Duct blaster+ Blower door
Subtraction technique	Blower door
Pressure pan technique	Blower door + Pressure pan
Delta Q techniques	Blower door

3.5 Field Test

For HVAC systems which have the air handler located in a closet or garage (easily accessible), the airflow through the air handler fan is measured by the method described in Annex A of ANSI/ASHRAE Standard 152-2004 [8]. Otherwise, the airflow through the air handler fan is measured by True Flow Air Handler Flow Meter. The True Flow manufactured by The Energy Conservatory is designed to provide a simple and accurate measurement of airflow through residential air handlers. It temporarily replaces the filter in the air handler distribution system during the airflow measurement process. If the filter location is directly adjacent to the air handler, the True Flow Meter will measure the total air handler flow. If the filter is located remotely at a central return, the True Flow Meter will measure airflow through the central return. When the air handler is located in an easily accessible closet or garage, a

barrier is used to separate the return and supply sides and the duct system is pressurized by the calibrated fan located at the air cabinet.

Figure 8. Duct Blaster installed in the air handling unit of house # 7

The duct blaster was installed in system located in the garage as shown in Figure 8. The supply and return ducts are separated using card board and the Duct Blaster is attached to the supply duct of the air conditioning by using duct tape as shown in Figure 9. All the sides of the card board connecting the air conditioning system were sealed neatly

using duct tape. No air should escape from the sides of the card board once the air is blown into the supply duct using the fan.

Figure 9. Duct Blaster installed in system to perform duct pressurization test

For house #8, the Duct Blaster was installed in the return register instead of placing it in the air handling unit itself because the units are located on the roof top. It is not easy to place the Duct Blaster in the unit itself. The Duct Blaster was connected to the return register by opening the return grill and placing the card board connecting the duct blaster to the return register as shown in Figure 10. The pressure probe is installed on the register that is nearest to the main supply duct; clear tape is used to block the register as shown in the Figure 11.

Figure 10. Duct Blaster installed in return register for house #8

Figure 11. Pressure probe installed on the register grill

The characteristics of the houses are listed in table 2. Details including the year built, area, installed cooling capacity, number of AHU, location of AHU, number of supply & return registers are listed.

Table 2. Characteristics of the houses #1-11

House ID	Year Built	Area of the House (Sq.ft)	Total installed cooling capacity (Ton)	Number of stories	Number of Air handling units	System type	Location of the air handler unit	Number of supply registers	Number of return registers
House#1	1993	1750	4.5	1	1	HP with electric heater	Attic	6	2
House#2	1994	1150	3	1	1	HP with gas furnace	Closet	7	1
House#3	1992	1400	4.5	1	1	HP with gas furnace	Attic	7	1
House#4	1990	2000	7	1	2	Air-conditioner with furnace	Attic	8	1
House#5	1990	2500	7	2	1	Air-conditioner with furnace	Garage	12	2
House#6	1992	3000	8.5	2	2	Air-conditioner with furnace	Attic	8	1
House#7	1988	3600	9.5	1	2	Air-conditioner with furnace	Garage	14	1

House#8	1980	3080	7	2	2	Air-conditioner with furnace	Attic	7	1
House#9	2005	1954	5	2	1	HP with electric heater	Attic	17	2
House#10	2001	1700	3.5	2	1	HP with electric heater	Attic	13	2
House#11	1993	2500	5.5	1	2	HP with electric heater	Garage	13	2

In the above table HP refers to Heat Pump.

Table 3 lists the airflow through the air handler and the operating pressures in the supply and return plenum. Pressure probes are used at the supply and return plenums to record the pressure difference between supply or return duct and the house. If the owner denies accepting to drill a hole in the supply/return duct, alternative locations such as the nearest registers may be used for pressure measurement.

Table 3. Airflow rate and operating pressures of Houses#1-11

House ID		Airflow through the air handler (CFM)	Operating pressure in the supply plenum (Pa)	Operating pressure in the return plenum (Pa)
House#1		1750	45	38
House#2		1252	28	30
House#3		1420	40	30
House#4		1150	55	38
House#5		2014	52	41
House#6		1324	37	28
House#7		2165	27	28
House#8		1354	15	19
House#9		1650	50	-
House#10		1300	48.5	-
House#11	AHU1	900	53	-
	AHU2	725	40	-

Due to time constraints, the testing techniques are applied only to one air handling unit (the larger system) for the houses that have two systems. The only exception is that the testing techniques are applied to both air handling units in House#11. The leakages measured at the test pressures are not equal to the actual leakage rates at the operating pressure unless the operating pressure happens to be 25Pa. The leakage at operating conditions is determined. In Table 4, the leakages measured

using duct pressurization technique are corrected by using the correction factor @ half pressure [18]. The formula used for correcting the leakage measured using duct pressurization technique is shown below.

In Table 4,

$$CF_2 = \left(\frac{Supply\ \Pr essure / return\ \Pr essure\ @\ Fan}{2 \times 25\ pa} \right)^{0.6} \qquad CFM_{Corr} = CFM_{dpt} \times CF_2$$

Table 4 shows the leakage measurements made in each home using the duct pressurization technique. The detailed supply and return leakages measured for houses # 1-11 are tabulated in table 5.

Table 4. Total leakages measured using the duct pressurization technique

House ID	Duct pressurization technique @ 25 Pa(cfm) CFM $_{dpt}$		Corrected duct pressurization values using actual supply pressure and return pressures at the fan(Using correction factor CF 2)CFM $_{corr}$	
	Supply	Return	Supply	Return
House#1	330	96	309.7	81.4
House#2	200	42	141.2	29.6
House#3	95	15	83	11
House#4	96	12	101.3	12.6
House#5	358	110	366.2	98
House#6	95	26	79.5	18.6
House#7	293	62	208.7	45
House#8	85	46	41.2	25.7
House#9	165	-	165	-
House#10	140	-	137.4	-
House#11	413	-	395.4	-

Table 5. Detailed supply/return local leakages measured by the proposed technique

House ID	Supply Leakage(cfm)	Return Leakage(cfm)
House#1	339.6	81.4
House#2	181	29.6
House#3	97.2	11.2
House#4	101	9.3
House#5	440	98
House#6	100.8	18.6
House#7	227.8	44.1
House#8	41.2	25.7
House#9	165	-
House#10	137.4	-
House#11	395.4	-

The details of the total number of zone bag tests performed are tabulated in Table 6. The decision regarding the number of zone bag tests to be performed is made by keeping in view of the "Reachability Factor". The research team could not insert the plastic hose pipe with the zone bag inflated completely into the duct at some locations in the houses tested. So the number of zone bag tests performed was limited.

Table 6. Number of zone bag tests performed for houses#1-11

House ID	**Number of zone bag tests performed**
House#1	3
House#2	4
House#3	4
House#4	4
House#5	4
House#6	2
House#7	3
House#8	2
House#9	4
House#10	4
House#11	2

The different techniques applied to the houses #1-11 are shown in Table 7. For houses 9, 10 and 11, the research team could not separate the supply and return duct, so the return leakage is not tabulated in tables for these houses. In these houses, the plenum could not be separated from the registers, so the data for the leakage in plenum, leakage in registers could not be tabulated.

Table 7. Leakage percentages measured in houses

House ID	Duct pressurization technique % leakage with respect to total flow		Delta Q technique % leakage with respect to total flow		Proposed technique % leakage with respect to total flow			
	Supply leakage	Return leakage	Supply leakage	Return leakage	Supply leakage	Return leakage	Leakage in plenum	Leakage in Registers
House#1	18.9	5.5	13	3.1	19.4	4.7	9.0	10.4
House#2	16.0	3.4	10.6	1.5	14.45	2.36	10.22	4.23
House#3	6.7	1.1	6.5	1.1	6.85	0.78	5.52	1.32
House#4	8.3	1.0	10.2	0.5	8.76	0.8	5.86	2.92
House#5	17.8	5.5	20.1	6.2	21.85	4.86	18.8	3
House#6	7.2	2.0	-	-	7.62	1.41	5.19	2.42
House#7	13.5	2.9	-	-	10.52	2.04	8.68	1.83
House#8	6.3	3.4	-	-	3	1.9	3	-
House#9	10.0	-	-	-	10	-	-	-
House#10	10.8	-	-	-	10.5	-	-	-
House#11	25.4	-	-	-	24.3	-	-	-

3.6 Duct Sealing

A local licensed HVAC contractor (Mojave Air) was hired to perform the sealing of the ducts in the four chosen houses. Four houses are selected based on several factors. Primarily the selection was made based on the leakage rate as a percentage of total flow in the house (i.e. higher percentage leakage we deemed better candidates), the home owner's willingness to allow fixing the leakages and retesting the house. These

were all considerations and limitations on what the research group can do. Hence the decision was made taking these considerations into account, to choose houses #5, 7, 8, and11.

Digital photos of the various aspects of the HVAC ducts found in Houses #5, 7, 8 and 11 are included. The houses were retested for leakage (at a later date) after sealing the ducts. The percentage improvement in the leakage reduction is noted. The aim is to reduce the leakage rate from these ducts as compared to the supply flow rate. The address and identity of the homes' owners are not presented here for privacy. It can be said that the locations of these homes are in the Las Vegas Valley.

3.7 Sealants

3.7.1 DP 1010

A smooth, water based, premium quality, high pressure/high velocity duct sealant for commercial and residential supply and return air duct is used for sealing purposes. It is shown in Figure 12. The technical data is provided by the manufacturer [19].

Figure 12. Smooth gray water based sealant used in duct sealing

Recommended Uses:

- Recommended for sealing joints, seams, and duct wall penetrations.
- Recommended for sealing connections on flexible duct.
- Recommended up to 15 inches water column pressure.

DP 1010 may be used to seal joints on metal, flexible and fiberglass duct board supply and return air duct.

- Surface Preparation: Surfaces should be clean, dry and free of dirt, oil and any foreign matter.
- For sheet metal duct: DP 1010 should be applied to all connections according to SMACNA standards. Brush, caulk, pump or trowel DP 1010 on all duct seams. Apply to TDC/TDF and applied flange corners. Apply to all penetrations in the duct wall including sheet

metal screw heads and tie rods. When caulking DP 1010, sealant should be brushed into seams.

- For flexible duct: Install flexible duct per manufacturer's instructions using draw bands or mechanical fastener. Apply DP 1010 between the end of the duct and the collar in a 2-inch band. Use DP 1010 to seal
- All connections of collar to metal duct or rigid fiberglass ductboard.

3.7.2 GE Window and Door Foam

GE Silicone window and door foam offers excellent performance in most applications. It is permanently flexible, and adheres to most woods, ceramics, glass, aluminum and steel.

Figure 13. Insulating foam sealant used in duct sealing

It provides a weatherproof and watertight seal. It is not recommended for masonry, concrete, stone, or oily woods. As shown in Figure 13, the blue and gray colored tin represents GE window and door foam. The applications and features are provided by manufacturer [20].

Applications:

Sealing interior and exterior windows, doors & vents, replacing window panes, sealing cracks in the door jams or window seals

Features:

- Indoor/outdoor
- Watertight
- Minimal shrinkage
- Remains flexible
- Strong adhesion to most surfaces: most woods, metals, plastics, glass, vinyl siding and drywall/plaster

3.7.3 Dow Great Stuff Insulating Foam Sealant

Great Stuff Gaps & Cracks is minimal expansion polyurethane insulating foam sealant that fills, seals and insulates gaps up to 1/2 inch. It expands to take the shape of cracks and voids to form a permanent, airtight, and water-resistant bond that eliminates unwanted airflow and helps reduce condensation. In Figure 13, the red colored sealant tin on the left side of the figure represents Dow Great Stuff insulating foam sealant. The features of the sealant are provided by manufacturer [21].

Features:

- Forms a permanent weather-tight seal to minimize drafts and insect infestation for gaps, cracks and holes less than ½ inch.
- Interior or exterior use.
- Exceptional adhesion to wood, drywall, metal, masonry, glass and most plastics.
- Airtight, water-resistant.
- Tack free in 6 minutes; Trims in 30 minutes.
- Foam elasticity allows for movement/shifting within a structure from winter to summer.
- Paintable, stainable and sandable.
- Cream colored foam.

3.8 Details of Houses with Ducts Sealed Using Sealants

House #5, 7, 8 and 11 are fixed for leakages in ducts. The leakage techniques used for the four homes discussed here are mentioned in Table 7.

Figure 14. Hole inside the insulation of the attic of house #5

A hole is seen located inside the insulation of the attic as shown in Figure 14. This hole was fixed with the help of the contractor. Figure 15 shows large gaps between the perimeter of the register boot and that of the drywall. The cut-out hole indicated a potential leakage to the outside.

Figure 15. Register opened to do the sealing job in house #5

Smooth gray water based sealant is used to fix the leaks inside the supply and return ducts. As shown in Figure 16, a register is sealed neatly using smooth water based sealant. A paint brush is used to apply the smooth water based sealant on the inner/outer layers of the duct.

Figure 16. Register Sealed neatly using smooth gray water based sealant in house #5

It is noticed that part of the duct connection to the boot of the register is closed partially to restrict the flow of air so as to balance the air flow for the entire system. This partial obstruction is not well observed in that image because that obstruction was painted black and did not reflect the light well to show its features as shown by the arrow in Figure 17. This was a correction that the initial HVAC contractor installed to improve the distribution the air flow to the different parts of the house.

Figure 17. Obstruction shield installed to improve air flow distribution in house #5

The registers were opened to fix the leakages. They were neatly sealed using the smooth gray water based sealant. The gaps between the drywall and the outer surface of the register are sealed neatly using the Insulating Foam Sealant as shown in Figure 18.

Figure 18. Register sealed neatly using Insulating Foam Sealant in house # 7

A gap was noted in between the supply duct and the boot connecting the return register as shown in Figure 19. Considerable amount of air leaked from the gaps as shown. It was sealed neatly by using an aluminum tape as shown in Figure 20.

Figure 19. Return register opened to do sealing job in house # 7

Figure 20. Return register sealed neatly using aluminum tape in house # 7

Some gaps were noted between the main duct and the air conditioning systems which are fixed by using the smooth water based sealant. It is applied evenly around the circumference of the duct by using a brush as shown in Figure 21.

Figure 21. Leakage sealed using smooth water based sealant

A gap was noted on the outer surface of the main duct and the boot connecting the air conditioning system inside the attic as shown by the arrow in Figure 22. It was fixed neatly by using aluminum tape around the circumference of the duct. As the hole was located very near to the air conditioning system outlet the amount of air lost through this hole is expected to be large due to the high pressure of air coming from the supply duct and large size of the hole.

Figure 22. Gap located on the outer surface of duct located in the attic ofhouse # 8

The schematic of air distribution system for house #7 is shown in Figure 23. The layout contains location of air handling unit, duct layout, location of supply registers, location of return registers, and location of zone bags.

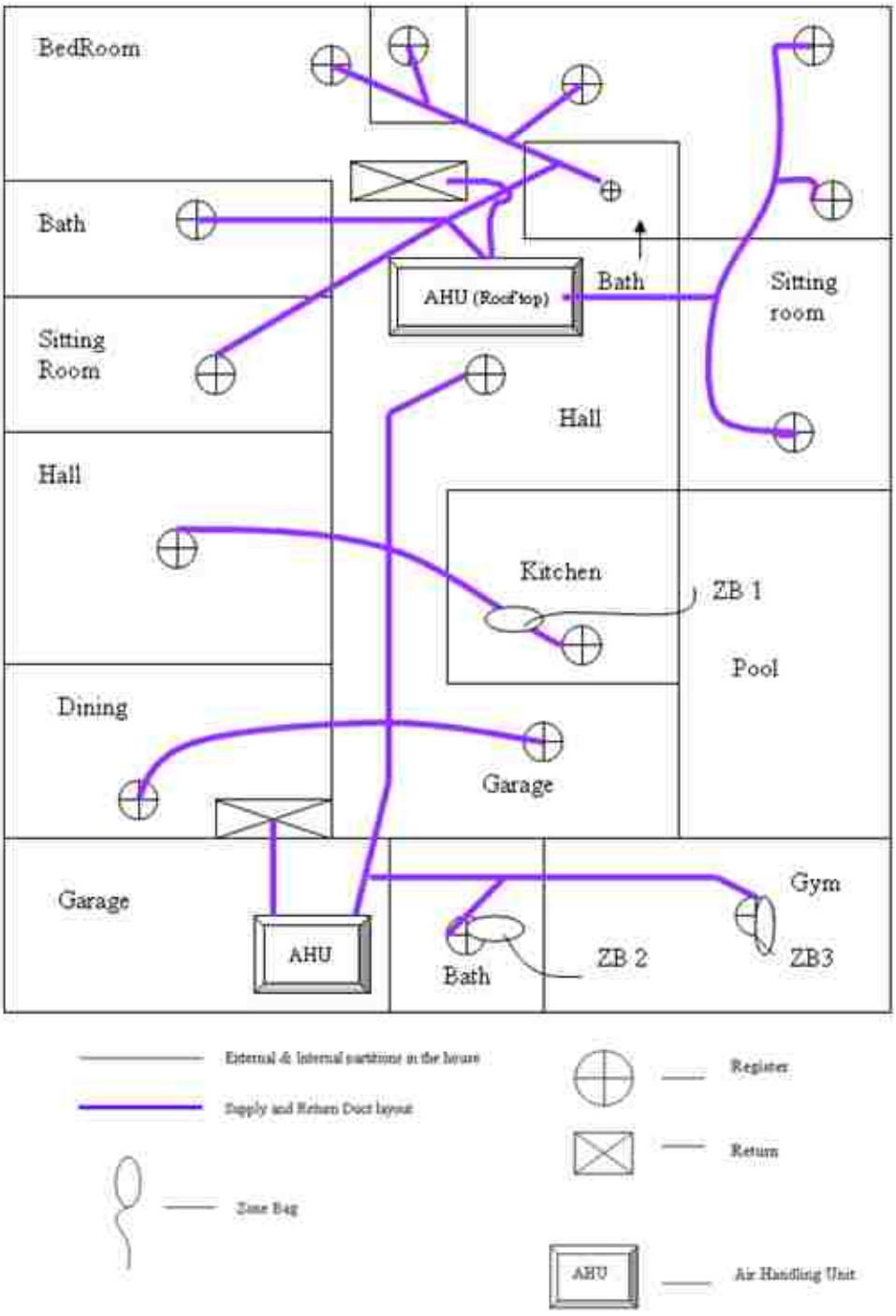

Figure 23. Schematic of the air distribution of house #7

The schematic of air distribution system for house #11 is shown in Figure 24. This house was built in 1993. The house had two air conditioning systems located in the garage as shown in the floor layout. The size of condensing unit supporting AHU 1 is 3.5 ton of refrigeration and condensing unit supporting AHU 2 is 2 ton of refrigeration.

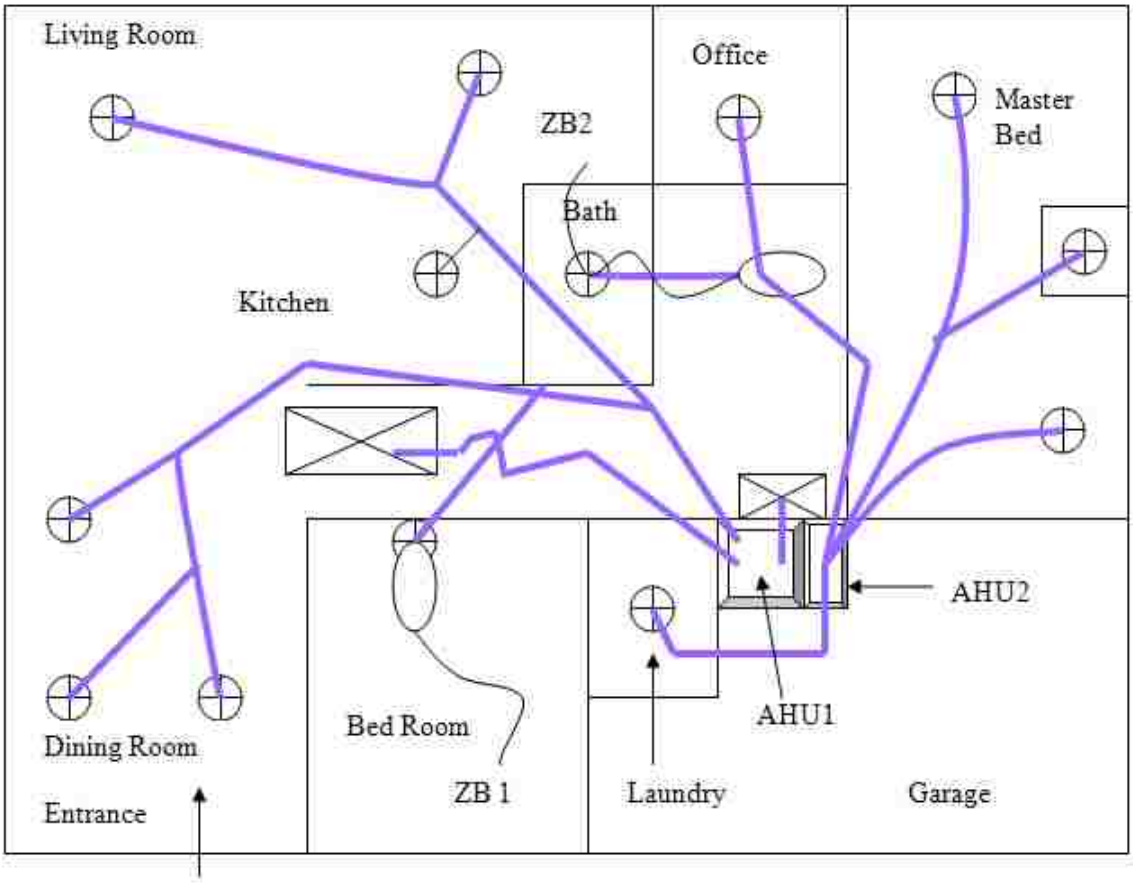

Figure 24. Schematic of the air distribution of house #11

3.9 Retesting Houses after Leak Repairs

After fixing these four homes, the homes are retested to assess the duct leakage reductions and benefits. The techniques discussed in Table 7 (except Delta Q) are applied again to these houses. The Delta Q technique is not applied due to time constraints. The zone bag technique applied to these houses is discussed in the final report [18].

3.10 Results

In table 8, the total leakages of the houses are compared using duct pressurization technique before and after fixing the leakages. A considerable amount of reduction in the total leakage is noticed. The total number of registers on the low level side and high level side of the zone bag are tabulated in table 9. In table 9, the sample of the total local leakage for selected houses using proposed technique is tabulated. It is noticed that the leakage in the specific zone (On lower level of the zone bag) is reduced significantly. The reduction is also observed on the higher level of zone bag. The number of zone bag tests could not be performed for the all registers due to “Reachability” problem faced by the research team. The total number of zone bag testing done for each home is shown in table 6.

Table 8. Total Leakages measured before and after fixing the leakages

House ID		Actual operating pressure(Pa)		Total supply air flow rate (cfm)		Total leakage Measured using DPT(cfm)		Leakage as percentage of total supply air flow. %		Total leakage percentage reduction (after fixing the leaks) with total initial leakage as reference %
		Before	After	Before	After	Before	After	Before	After	
House#5		52	52	2014	2014	468	300	23.3%	15%	35.8
House#7		55	80	2165	2220	355	190	16%	8.6%	46.5
House#8		31	31	1354	1354	131	110	9.7%	8.1%	16
House#11	AHU1	53	60.5	900	905	208	178	23.1%	19.7%	14.4
	AHU2	40	45	725	805	205	140	28.3%	17.3%	31.7

Table 9. Sample of total local leakages measured for selected houses by using proposed technique

House ID		Total leakage(supply leak + return leak) measured using proposed technique (cfm)				Total number of registers	
		Before fixing the leaks		After fixing the leaks			
		Low level leak	High level leak	Low level leak	High level leak	On low level side	On high level side
House #5		169.6	298.4	53.3	246.7	6	6
House #7		134	221	4.3	185.7	3	4
House #8*		-	-	12.5	97.5	3	4
House #11	AHU1	10	198	3.8	174.2	3	3
	AHU2	6.3	198.7	5	135	2	4

The results obtained here are compared with the report obtained from Nevada Power [22]. The only other study which was made in regards to leakage reduction was a measurement and verification (M&V) study was conducted to quantify electrical energy consumption and peak demand reductions achieved as part of the Nevada Power Company Air Conditioning (AC) Rebate Program during the summer of 2004. In the Nevada Power report it is noted that the overall results show that the AC duct seal jobs resulted in reductions in energy usage and hourly average demand of between 13% and 9% respectively. It is also noted that the leakage rate for different houses could be decreased from 14.4% to 46.5% of the total initial leakage rate. The total leakage rate can be decreased by 2 % to 11 % of the total initial supply air flow rate. This means that the energy usage could be reduced by 2% to 11%, depending on the individual house. The houses chosen for the NP study were not the same as those in this study and their numbers (6 Homes) were not large enough to deduce a clear statistical inference for the advantages/disadvantages of each approach to reducing the duct leakage rates.

Through private conversations with the only franchisee of the Aeroseal technology in the Las Vegas area it was found that the estimated cost for sealing a home with that technology is around $2,000

per typical home. This figure is much larger than what has been experienced by this study as seen in the Table 10.

3.11 Cost Incurred For Fixing the Leakages

The costs involved in sealing the ducts are calculated; a record is presented of the costs involved in sealing these four homes which represents a small sample of typical homes in the Las Vegas Valley. The total billed man hours are also reported here for each job. The total savings and simply pay back are calculated by assuming the annual power bill for the houses is $3000 per year.

Table 10. Costs incurred in fixing the leaks

House Number	Man Hours	Cost incurred for testing the house	Cost incurred to fix the leaks in the house	Total Cost	Savings Per year $ (Total leak reduction percentage *3000)/100		Simple pay back (Years)
House # 5	8.0	350 $	657 $	1007 $	249$		4
House # 7	7.0	300 $	577 $	877 $	222$		4
House # 8	3.0	200 $	253 $	453 $	48$		9.4
House # 11	2.5	200 $	215 $	415 $	AHU1	99	1.1
					AHU2	240	

CHAPTER 4

CFD MODELING OF HVAC MIXING BOX

4.1 Mixing box

Mixing box is an important component of the heating ventilating and air conditioning (HVAC) delivery unit. Because of its vital role in HVAC system and widespread application, it is selected as the component to be investigated to find out if a CFD analysis can provide quantitative predictions as well. A mixing box is the section of an air handling unit used to mix the return air flow with the outside air flow. Return air as in [23] is supplied from the top of the box and outside air supplied from the back of mixing box as shown in Figure 25.

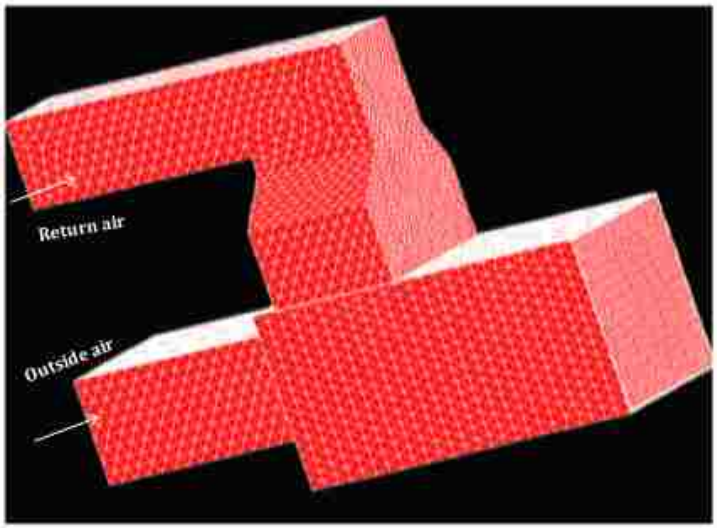

Figure 25. HVAC mixing box

Fresh air is introduced in the outside air duct in order to lower the amount of contaminants in the building. Improper mixing of air can mainly occur due to lack of mixing [24]. Stratification in ventilation ducts is a common problem in areas that have cold winters. It occurs when the warm return air and the cold outdoor air do not mix properly and lead to a number of problems. The most severe effects are unit shutdowns due to low limit thermostats, frozen coils [25] and sensor errors [26]. Methods to detect HVAC sensor faults have been suggested by Yang and Jiang [27] and by Wang and Wang [28].

So far, measurements and simple models are used to study the conditions in mixing boxes. Computational fluid dynamics (CFD) regarding ventilation ducts has mostly been used for calculation of pressure losses. CFD provides a convenient tool to study temperature stratification as well. Par Carling's paper presents a comparison between CFD simulations and measurements of the temperature stratification in an AHU mixing box [23]. A two-dimensional CFD model is used in his study. In this thesis a three-dimensional mixing box model is constructed based on the dimensions from the paper published in International Journal of Energy Research [23]. The objectives of this study is to examine if CFD 3-D modeling will improve the theoretical predictions with respect to the experimental results [23] and shed some light on the effect of air leakage into the duct at the mixing box location.

4.2 CFD modeling

CFD modeling is a process of representing a fluid flow problem by mathematical equations based on the fundamental laws of physics, and solving those equations to predict the variation of relevant parameters within the flow field. Usually these will be velocity, pressure and temperature and other variables such as concentrations of typical pollutant species [29] [30].

4.2.1 STAR-CD

STAR-CD is commercially available software for computational fluid dynamics (CFD) which is marketed by CD-adapco. It is widely used in many sectors of industry and academia. It is based on the finite volume method. STAR-CD is a multipurpose thermal fluid analysis code. The solver provides numerical model solvers for both steady state and transient simulations. STAR-CD incorporates mathematical models of a wide range of thermo fluid phenomena including steady and transient; laminar and turbulent, incompressible and compressible. The mass and momentum conservation equations are solved by STAR-CD for general incompressible fluid flows in Cartesian tensor notation. Star CD offers extensive capabilities for viewing the results of the CFD analysis. The graphical output can be generated in the form of vector plots, contour plots, particle tracking, and graphs.

4.2.2 High Reynolds Number k-ε Model

High Reynolds number k-ε Model for turbulent flow is used. The k-ε high Reynolds number model (used here) in Star CD comprises of transport equations for the turbulent kinetic energy, k, and the dissipation rate, ε. (STAR CD user manual) .These two transport equations are described in Equations 5 and 6, respectively.

The governing equations describing conservation of mass, momentum and energy are described using conservative equation variables and are described using tensor notation in Equations 1, 2 and 3.

Conservation of Mass

$$\frac{\partial \rho}{\partial t} + \frac{\partial}{\partial x_j}(\rho u_j) = s_m$$	1

Conservation of Momentum

$$\frac{\partial \rho u_j}{\partial t} + \frac{\partial}{\partial x_j}(\rho u_j u_i - \tau_{ij}) = -\frac{\partial p}{\partial x_i} + s_i$$	2

Where:

t = time

x_i = Cartesian coordinate

u_i = velocity components

p = piezometric pressure

ρ = density

τ_{ij} = stress tensor components

s_m = mass source

s_i = momentum source components

Conservation of Energy

$$\frac{\partial \rho h}{\partial t} + \frac{\partial}{\partial x_j}(\rho h u_j + F_{h,j}) = \frac{\partial p}{\partial t} + u_j \frac{\partial p}{\partial x_j} + \tau_{ij} \frac{\partial u_i}{\partial x_j} + s_h$$	3

Where:

$$h = \overline{c_p} T - c_p^0 T_0 + \sum Y_m H_m = h_t + \sum Y_m H_m$$	4

T = temperature

Y_m = mass fraction of mixture constituent m

H_m = heat of formation of constituent m

c_p = mean constant – pressure specific heat at T

c_p^0 = reference specific heat at temperature T_0

$F_{h,j}$ = diffusional energy flux in direction x_j

s_h = energy source

h_t = thermal enthalpy

$$\frac{\partial}{\partial t}(\rho k) + \frac{\partial}{\partial x_j}\left[\rho u_j k - \left(\mu + \frac{\mu_t}{\sigma_k}\right)\frac{\partial k}{\partial x_j}\right] = \mu_t (P + P_B) - \rho\varepsilon - \frac{2}{3}\left(\mu_t \frac{\partial u_i}{\partial x_i} + \rho k\right)\frac{\partial u_i}{\partial x_i} + \mu_t P_{NL}$$	5

$$\frac{\partial}{\partial t}(\rho\varepsilon)+\frac{\partial}{\partial x_j}\left[\rho u_j\varepsilon-\left(\mu+\frac{\mu_t}{\sigma_\varepsilon}\right)\frac{\partial\varepsilon}{\partial x_j}\right]=$$ $$C_{\varepsilon 1}\frac{\varepsilon}{k}\left[\mu_t P-\frac{2}{3}\left(\mu_t\frac{\partial u_i}{\partial x_i}+\rho k\right)\frac{\partial u_i}{\partial x_i}\right]+C_{\varepsilon 3}\frac{\varepsilon}{k}\mu_t P_B-C_{\varepsilon 2}\rho\frac{\varepsilon^2}{k}+C_{\varepsilon 4}\rho\varepsilon\frac{\partial u_i}{\partial x_i}+C_{\varepsilon 1}\frac{\varepsilon}{k}\mu_t P_{NL}$$	6

Where:

$$P=S_{ij}\frac{\partial u_i}{\partial x_j}$$	7

$$P_B=-\frac{g_i}{\sigma_{h,t}}\frac{1}{\rho}\frac{\partial\rho}{\partial x_i}$$	8

$$P_{NL}=-\frac{\rho}{\mu_t}\overline{u_i' u_j'}\frac{\partial u_i}{\partial x_j}-\left[P-\frac{2}{3}\left(\frac{\partial u_i}{\partial x_i}+\frac{\rho k}{\mu_t}\right)\frac{\partial u_i}{\partial x_i}\right]$$	9

$$\mu_t=f_\mu C_\mu^{3/4}\rho k^{1/2} l$$	10

$\sigma_{\varepsilon =}$ turbulent Prandtl number

$C_{\varepsilon 1}$, $C_{\varepsilon 2}$, $C_{\varepsilon 3}$, $C_{\varepsilon 4}$ are coefficients whose values are listed in Table 11. These values were used as the default values suggested by the STAR-CD user manual [31] as no other experimental data was available to fine tune these values.

Table 11. Coefficients of the standard k – ε turbulence model

C_μ	σ_k	σ_ε	σ_h	σ_m	$C_{\varepsilon 1}$	$C_{\varepsilon 2}$	$C_{\varepsilon 3}$	$C_{\varepsilon 4}$	κ	E
0.09	1.0	1.22	0.9	0.9	1.44	1.92	1.44	-0.33	0.419	9.0

4.3 Model Description

A three-dimensional model of mixing box is developed with its dimensions obtained from the previous work [23]. The dimensions of the mixing box are shown in Figure 26. Air acts as the working fluid in this model. Return air is supplied from the top of the mixing box. The outside air is supplied from the back of the mixing box. The molecular properties of air are shown in Table 12.

Table 12. Molecular Properties of Fluid

Density	1.205 kg/m^3
Molecular viscosity	1.81x10^{-5} kg/ms

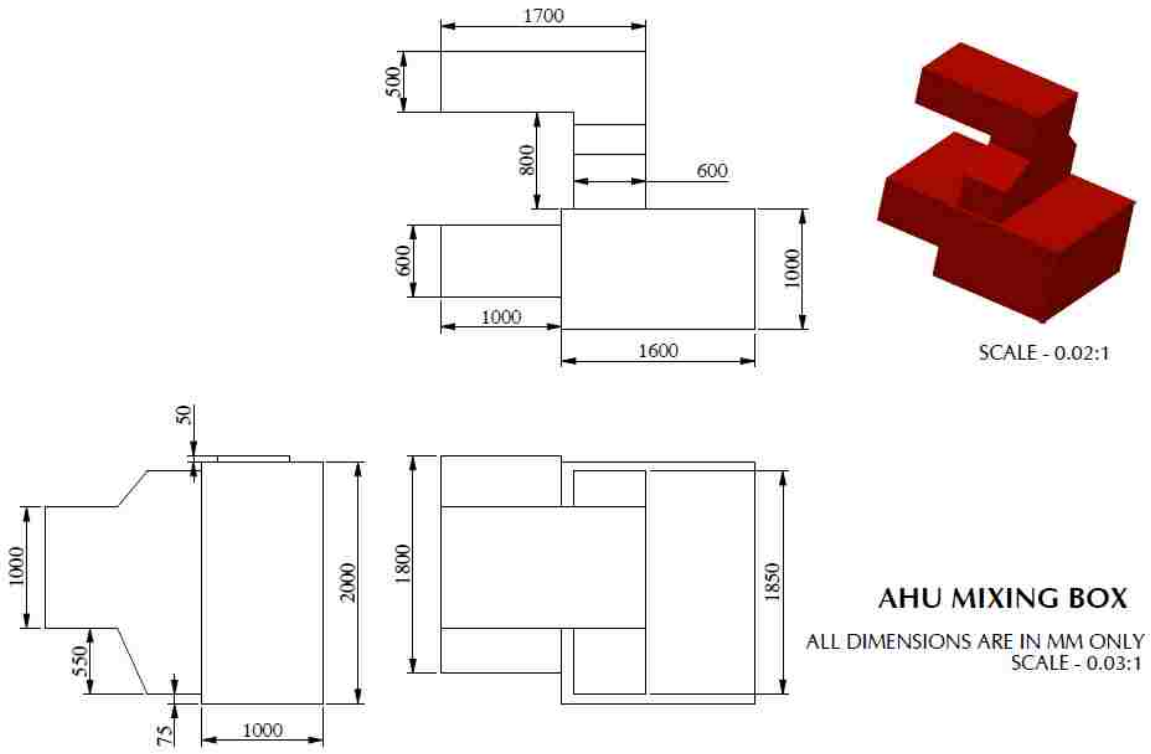

Figure 26. Dimensions of mixing box

Leakage in the HVAC ducts can be significant. This can result due to poor installation / tear in the duct. One such case is considered for study. An artificial leakage of 1.5 feet is introduced in the mixing box as shown in figure 27. Carbon dioxide enters the mixing box from the leakage. The effect of pollutant in the mixing box is also evaluated.

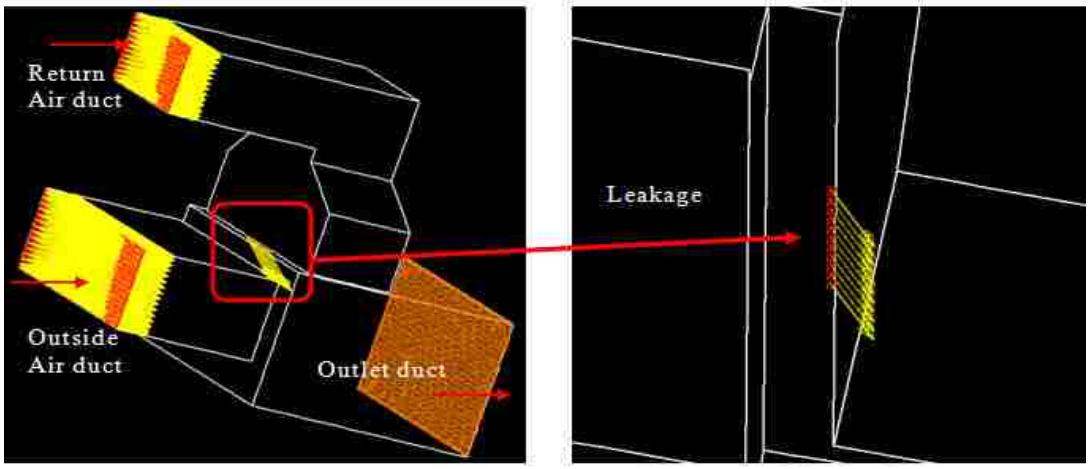

Figure 27. Mixing box showing inlet, outlet ducts and leakage

Par Carling used a two-dimensional CFD model of the mixing box to analyze the temperature and velocity profiles. The discrepancies between the experimental data and the two-dimensional CFD analysis data is considerable. Also, he did not consider any experimental accuracy in his CFD simulations. In this thesis, we considered a three-dimensional CFD model to better simulate a physically realistic model. Experimental accuracies are also considered on both temperature and velocities of return air and outside air. Further, the effect of carbon dioxide on the mixing is also analyzed.

Simulations are run for four different outside temperatures (-15 ° C, -5 ° C, 5 ° C, 15 ° C). The return air temperature remains constant at 23 ° C. The percentage of carbon dioxide concentration in outside air remains constant at 0.03% for all runs. Table 13 lists the simulations run for this model without considering the leakage in the mixing box.

Table 13. Simulations run without considering the leakage

Temperature	**Using the values from experimental data**	**Considering the uncertainty estimated on temperature**	**Considering uncertainty estimated on temperature and velocity**	**Number of simulations**
-15 ° C	♦	♦	♦	3
-5 ° C	♦	♦	♦	3
5 ° C	♦	♦	♦	3
15 ° C	♦	♦	♦	3

In the above table "♦" represents the simulation performed. Table 14 lists the simulations run for the model by considering the leakage. As shown in the table, the boundary conditions are modified by taking accuracy considerations on mass flow rates and temperatures. Using these modified boundary conditions simulations are run. The amount of carbon dioxide concentration from the return air duct is varied as shown in table. Three different carbon dioxide concentrations are introduced into the mixing box. The percentage of carbon dioxide concentration for outside air and the leakage is kept constant at 0.03%.

Table 14. Simulations run for the model by considering the leakage

Temperature	Percentage of carbon dioxide concentration in return air		Number of simulations
-15 ◦ C	0.04	♦	3
	0.06	♦	
	0.08	♦	
-5 ◦ C	0.04	♦	3
	0.06	♦	
	0.08	♦	
5 ◦ C	0.04	♦	3
	0.06	♦	
	0.08	♦	
15 ◦ C	0.04	♦	3
	0.06	♦	
	0.08	♦	

The temperature, velocity, carbon dioxide profiles of air are plotted. These plots are presented by taking the contours at the center section plane ABCDE (section slice) of the mixing box.

4.3.1 Boundary Conditions

The boundary conditions used to perform the CFD analysis are tabulated as shown in Tables 15, 16, and 17. For all the simulations the return air temperature is 296K (295.4K with accuracy considerations). The estimated velocities are found by using the estimated mass flow rates obtained from the field data [23]. Accuracy error considerations on mass

flow rates as well as temperature accuracy measurements are taken into consideration. The effect of accuracy considerations on the solution in analyzed. Table 15 shows the boundary conditions imposed on outside air temperature. The values of uncertainty are also listed in this table. Simulations are performed for the revised values of outside air temperature.

Table 15. Boundary conditions imposed on outside temperature

Outside Air Temperature (K)		
Mean value reported **a**	**Uncertainty from exp. data** **[Par Carling et al. 2001]** **b**	**Revised value used in 3-D model** **c**
258	+/-0.8	258.8
268	+/-0.8	268.8
278	+/-0.8	278.8
288	+/-0.8	288.8

Table 16 shows the boundary conditions imposed on the velocity of the return air. The percentage of uncertainty is also considered. Simulations are performed using revised values of velocity. Table 17 shows the boundary conditions imposed on the velocity of outside air. The percentage of uncertainty is also considered. Simulations are run using revised values of velocity.

Table 16. Boundary conditions imposed on velocity of return air

Outside air temperature (K) a	Velocity of Return Air		
	Mean value calculated (m/s) d	% of uncertainty estimated [Par carling et al. 2001] e	Revised velocity due to exp. accuracy considered in 3-D model (m/s) f [d + (d × e)]
258	1.8	27.2 %	2.29
268	2.12	30.7%	2.77
278	2.12	30.7 %	2.77
288	1.95	50.7 %	2.94

Table 17. Boundary conditions imposed on velocity of outside air

Outside air temperature (K) a	Velocity of outside Air		
	Mean value calculated (m/s) g	% of uncertainty estimated [Par carling et al. 2001] h	Revised velocity due to exp. accuracy considered in 3-D model (m/s) i [g – (g × h)]
258	1.81	16.6%	1.51
268	1.66	18.1%	1.36
278	1.58	18.9 %	1.28
288	1.58	32.9 %	1.06

The following assumptions are made for the simulation:

- The inner surface of the duct is assumed to be smooth, adiabatic and with a no slip condition.
- The air flow properties are considered to be isothermal (293K), incompressible and turbulent.
- The inlet velocity is axial with the cross flow components set to zero (except for the simulations with leakage).
- The molecular properties of the fluid are standard air properties (Density = 1.205kg/m^3. Molecular viscosity = $1.81x10^{-05}$ kg/ms).

4.4 Methods

4.4.1 Modeling

CAD software Pro/ENGINEER is used to model the HVAC mixing box. Pro/ENGINEER is a parametric, integrated 3-D CAD/CAM/CAE solution created by Parametric Technology Corporation (PTC) [32]. The dimensions of the mixing box are obtained from the paper published in [23]. In that paper, a 2-D model of the mixing box is used for simulations. A more physically realistic three-dimensional model is considered in this thesis. After building the CAD model, file is saved in the form of an *.iges file.

4.4.2 Meshing

HyperMesh 9.0 is used to generate grids in the model. HyperMesh is high-performance finite element pre-processor that provides a highly interactive and visual environment to analyze product design performance. Its features include high speed, high quality meshing. The *.iges file generated by using Pro/E is imported into hyperMesh. The CFD profile is selected as environment. Tetrahedral grids are generated for this model. A boundary layer is created along the outer surface of mixing box. It consists of five layers of fine meshes with increasing thickness. This allows us to capture the rapid changes of velocity in the boundary layer region. A smooth transition ratio is used there by optimizing the mesh quality as shown in Figure 28.

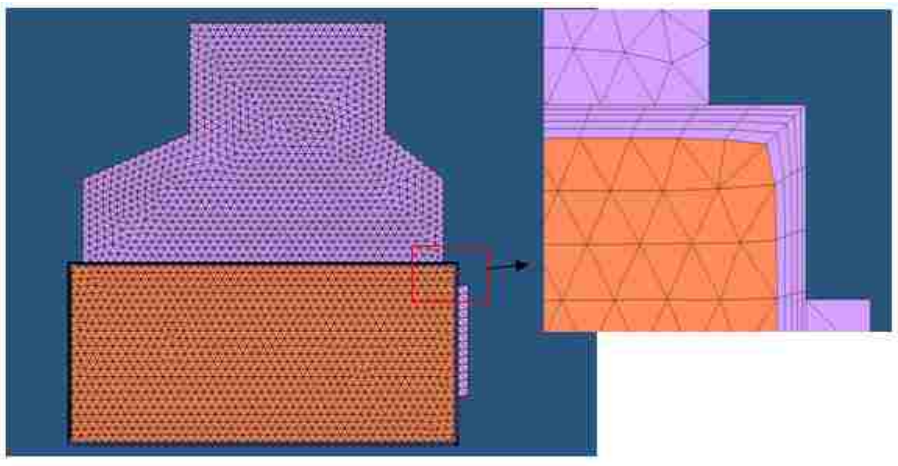

Figure 28. Mesh showing the boundary layers along the outer surface of mixing box

4.4.3 Analysis and Post Processing

The CFD analysis of the mixing box is done using Star CD 3.24. The model meshed in hypermesh is saved as a Nastran file and is imported to StarCD. The properties that will dictate the fluid flow are defined. The boundaries of the flow regime are specified according to the nature of the problem along with the physical properties of the fluid. The use of user subroutines is also available if non-constant conditions might exist in the flow (i.e. changing thermal properties, density, heat flux, etc.). These can be implemented using FORTRAN coding. SIMPLE is the solution algorithm used here. It is the default option and works well for most steady state solutions [31].

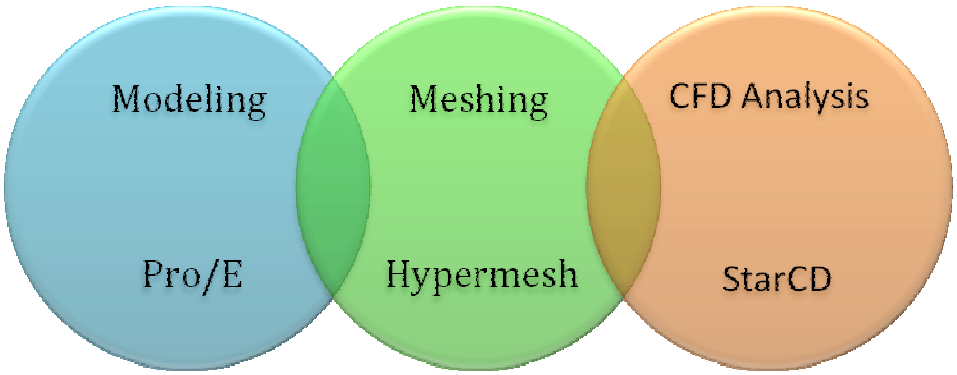

Figure 29. The overview of all the methods and codes used in this analysis

Post processing allows the user to view the results after running the simulation (after a convergence criterion is satisfied). Graphs, contours, and particle tracks can be created using post processing functions. An overview of all the methods and software used in this analysis is shown in Figure 29.

CHAPTER 5

RESULTS AND DISCUSSION

5.1 Grid independency

A grid independency test was performed on the model to determine the optimum size of the cell. The effect of cell density on the results was determined. The accuracy of the solution depends upon the size of the cell. The accuracy of the solution is decreased when a coarse cell is used for the solution. Therefore finer cells are used to perform the analysis.

The numbers of elements in this model are increased by varying the size of the element. As the number of elements in the model increases the size of the grid becomes finer. Ideally, a mesh that can deliver the results with desired accuracy (approximately 1-3% change in a typical variable value between consecutive grid sizes) is sought. Five different meshes are built in HyperMesh to determine the ideal size of the element. These meshes are differentiated based on the number of elements in the model. Table 18 shows lists the number of elements generated in each mesh.

Table 18. Number of elements in the model

Mesh	Number of elements
a	167,000
b	217,000
c	346,000
d	454,000
e	552,000

The solution is monitored for any changes in the parameters such as temperature and velocity. The temperature readings are taken along the central axis E-E (horizontal) of the outlet duct surface shown in figure 30. These sample values are compared with each other by varying the size of cell.

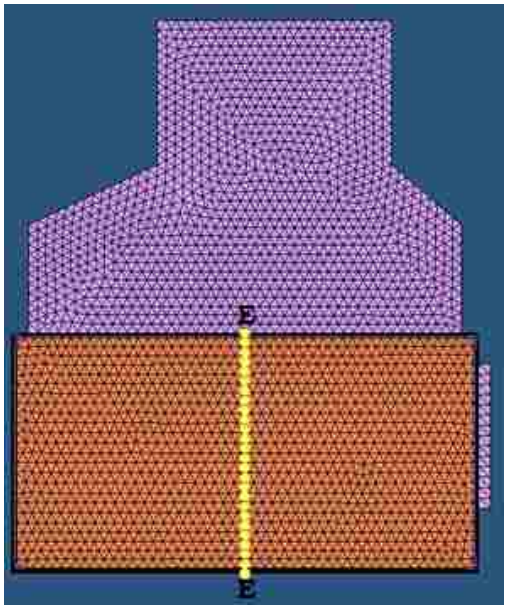

Figure 30. Central axis E-E taken along the outlet of the duct surface

The grid independency test is performed for outside temperature of -15 ° C, as the mesh size that is finalized can be used for all other temperatures. Results with the desired accuracy can be obtained by using the finalized mesh for all other boundary conditions. The grid independency plot showing all five meshes with temperature plot is shown in Figure 31. The difference between the temperature readings of the two meshes for 454K and 552K is less than 1%. So 552K mesh is used finally for producing all productive runs.

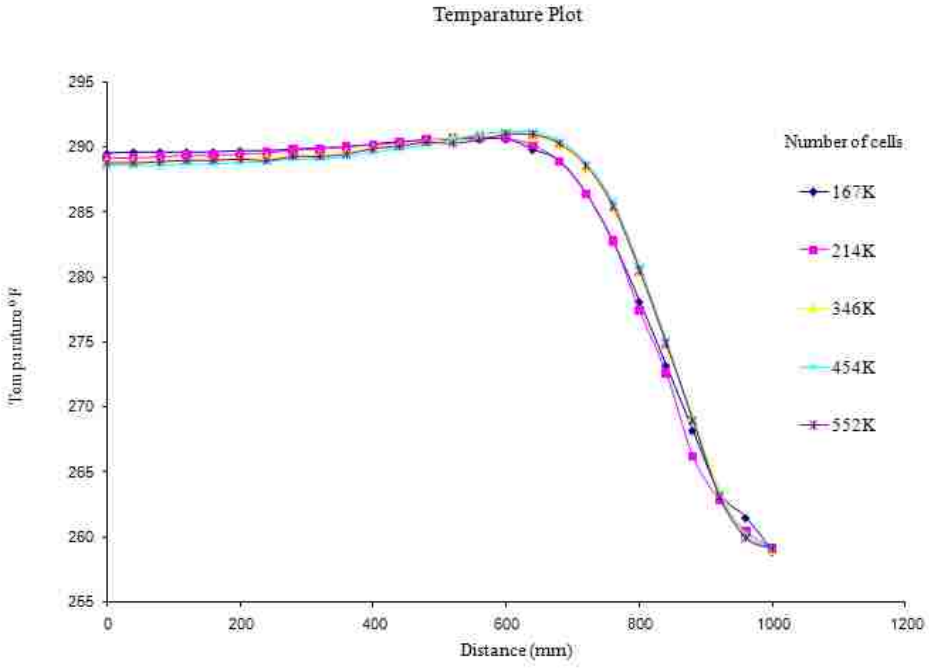

Figure 31. Grid Independency plot showing temperature readings

The grid independency plot showing all five meshes with velocity plot are shown in Figure 32. The difference between the velocity readings of the two meshes for 454K and 552K is less than 2%.

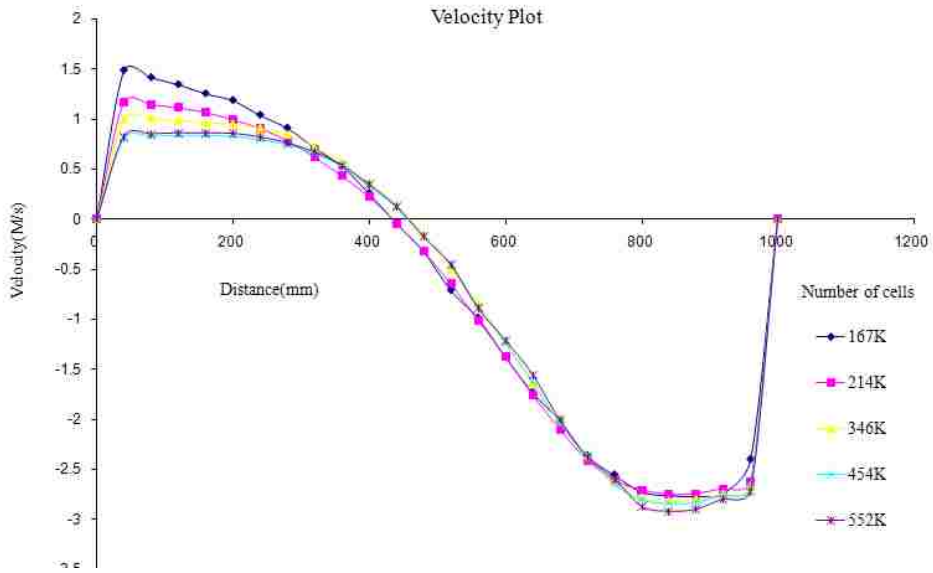

Figure 32. Grid independency plot showing velocity readings

As the number of cells increases, the computational time is increased. The computational time and computational memory can be optimized by selecting an optimum size for mesh.

5.2 CFD Simulation

STAR-CD is used to predict the air flow/temperature 3-D distributions in the mixing box. By applying the boundary conditions to the model, the temperature, velocity and carbon dioxide profiles of the mixing box are

then plotted. Simulations are run for four different outside temperatures (-15 ° C, -5 ° C, 5 ° C, 15 ° C). The return air temperature is 23 ° C for all simulations.

The temperature distribution inside the mixing box is shown in Figure 33. Average measured values for temperature and velocity inputs are considered for this simulation result. The outside air temperature is -15 °C and the return air temperature is 23 °C. Figure 34 shows the display plane ABCDE profile plotted at the center axis (section slice) of the mixing box. This plane will be used to plot the temperature, velocity and carbon dioxide profiles of representative mixing box variables in the remainder of the thesis.

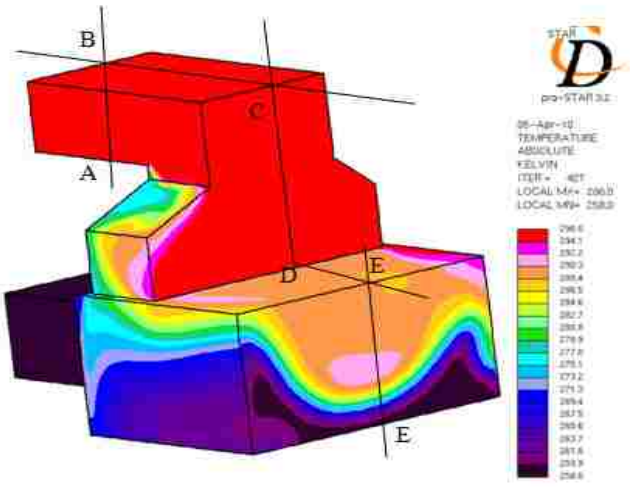

Figure 33. Temperature distribution with -15 °C of outside air

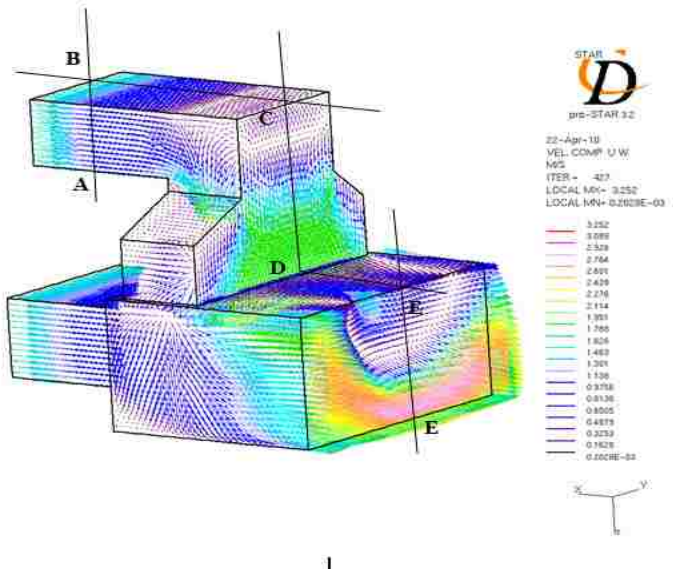

Figure 34. Velocity distribution with -15 ^{o}C of outside air

5.3 Simulations Run With No Leakage Consideration

Simulations are first performed without considering leakage on the suction side of the mixing box. Simulations are run using:

1) Input data are calculated by using experimentally measured average flow and temperature

2) Input data are then calculated by considering the experimental uncertainty in temperature measurements

3) Input data are then calculated by considering the uncertainty in flow and temperature experimental data

5.3.1 Experimentally Measured Flow Rate and Temperature

Figure 35 shows the temperature profile of the mixing box at the middle section plane ABCDE (slice). The outside air enters the mixing box at a temperature of -15 ^{o}C. The return air temperature enters the mixing box at a temperature 23 ^{o}C. Return air temperature is maintained at 23 ^{o}C for all the simulations (except for the simulations considering the uncertainty). The experimental data [23] are used to run the simulations. The simulations are performed without considering any accuracy considerations on the temperature and velocity of both the return and outside air. The return air mixes with the outside air at the center of the mixing box. High temperatures are noticed at the top of outlet duct when compared to the lower end of the outlet duct (column II of Table 19). The temperature of the mixed air at the end of the outlet duct increases from bottom to top.

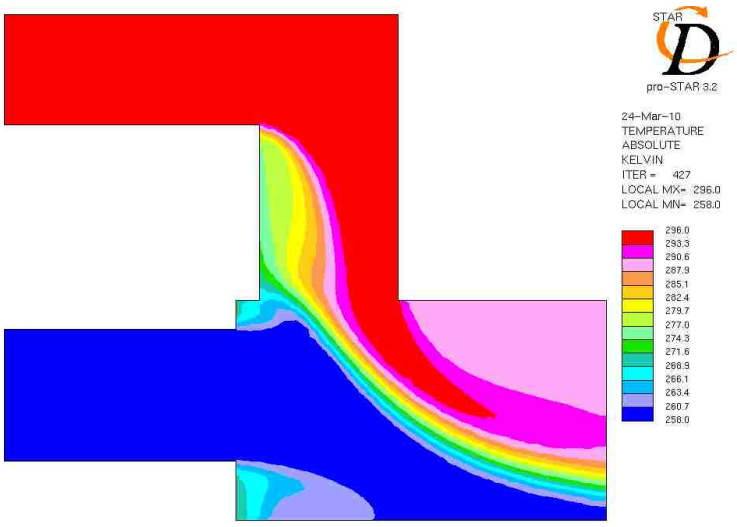

Figure 35. Temperature profile of section ABCDE with -15 °C of O.A

Figure 36 shows the velocity profile of the mixing box at the middle section plane ABCDE (slice). The velocity of the outside air is 1.81 m/s and the velocity of return air is 1.8 m/s. The air velocities at the entrance of the inlet ducts are assumed to be uniform for the simulations. The return air stream mixes with the outside air stream at the center of the mixing box. An abrupt expansion of the outside air duct area is noticed in the mixing box. This results in shock losses. For practical applications, the velocity distribution over the conduit length upstream of an abrupt expansion is, as a rule, never uniform [33]. The velocity of the outside air is not uniformly distributed at the center of the mixing box. The velocity decreases as the outside air enters the expanded section of the mixing box.

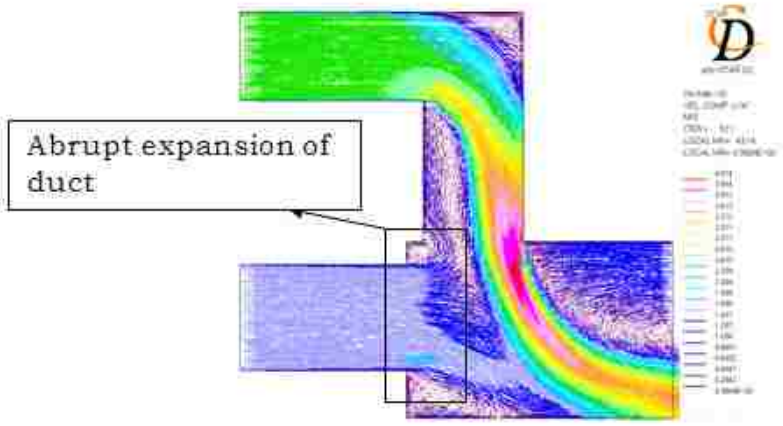

Figure 36. Velocity profile of section ABCDE with -15 °C of O.A

Figure 37 shows the temperature profile at the middle section (slice) of mixing box at 15 ^{o}C of outside air. Return air is supplied at 23 ^{o}C .No accuracy considerations are considered for this simulation. A hot stream of return air drops down the return air duct to meet the outside air, thereby forming a contour of uneven temperatures. Heat is transferred from the hot air to the cold air which results in formation of mixed air at the outlet of the mixing box. The temperature of the mixed is not uniform as the return air and outside air are supplied at different velocities. This results in a considerable difference in temperature between the upper and lower part of the outlet duct of the mixing box. Figure 38 shows the velocity profile at the middle section plane ABCDE (slice) of the mixing box at 15 ^{o}C of outside air. Return air is supplied at a velocity of 1.95 m/s and outside air is supplied at a velocity of 1.58 m/s.

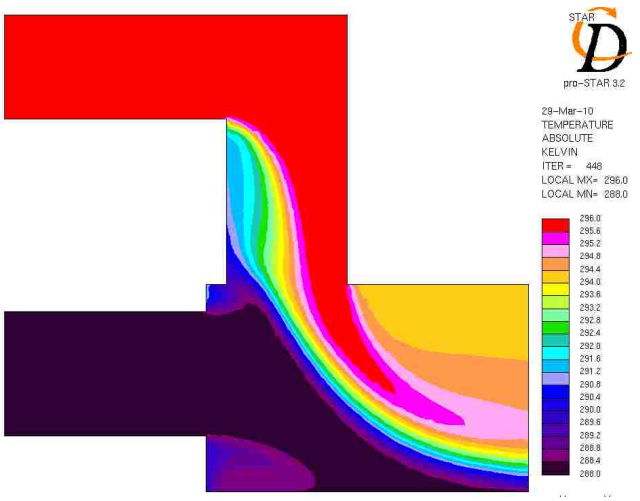

Figure 37. Temperature profile of section ABCDE with 15 °C of O.A

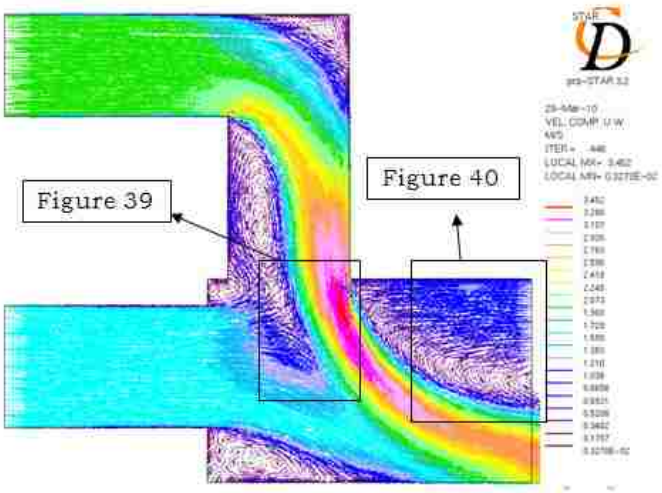

Figure 38. Velocity profile of section ABCDE with 15 °C of O.A

Air is drawn back into the mixing box at the outlet of the duct as shown in Figure 39. This creates turbulence at the outlet of the mixing box. There by increasing the load on the supply fan. The mixing

effectiveness of the mixing box at the outlet duct is affected. Therefore, the difference in the temperatures between the upper and lower parts of the mixing box at the outlet duct is increased.

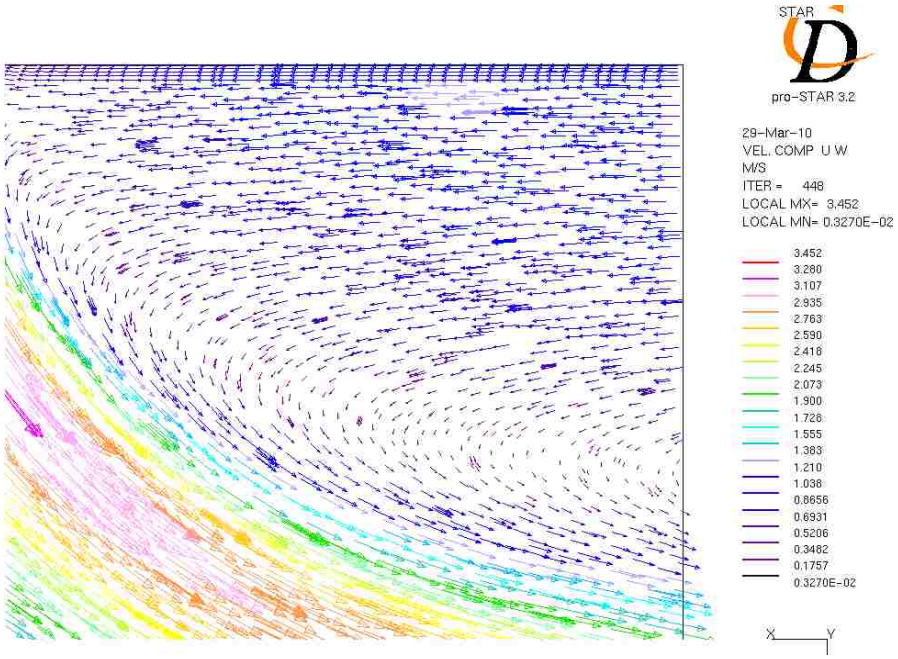

Figure 39. Air drawn back into the mixing box at the outlet duct

Hot air and cold air are mixed at the center of the mixing box as shown in Figure 40. Eddies are formed at various sections of mixing box. We observe that eddies overlap in space and large eddies carry smaller eddies. Turbulence features a cascade process whereby, as the turbulence decays, its kinetic energy transfers from larger eddies to smaller eddies [34]. Two steams of hot air and cold air moving in same direction but with different velocities merge, turbulent mixing of streams

usually occurs, which is accompanied by non recoverable pressure losses. In a course of this mixing, momentum exchange takes place between the particles of medium moving with different velocities. This exchange favors equalization of the flow velocity field. In this case, the jet with higher velocity loses a part of kinetic energy by transmitting it to the slower moving jet [33].

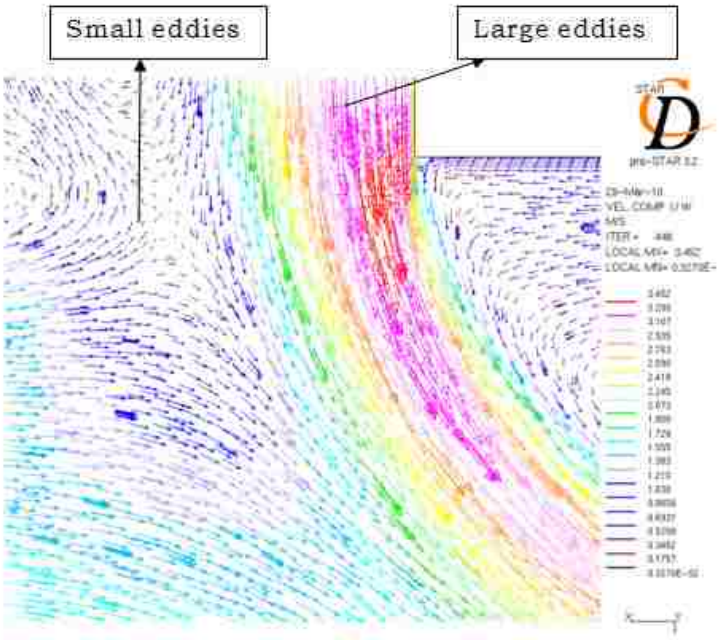

Figure 40. Velocity profile at the center of the mixing box

5.3.2 Experimental Uncertainty in Temperature

Figure 41 shows the temperature profile of the mixing box at -15 ^{o}C of outside air. The data of this plot consider the uncertainty estimated on both return air temperature and outside air temperature. In order to

provide a more physically realistic model, simulations are run by considering the uncertainties involved. By taking these considerations into account, the 3-D simulation results provide a better agreement with the experimental results. In this case, accuracy considerations are taken on the return air temperature and outside air temperature only, assuming that the velocity data taken from the experimental data is accurate as measured. The outside air enters the mixing box at a temperature of 258.8 K. Return air enters the mixing box at a temperature of 295.4 K. The temperature difference between the upper and lower part of the duct is reported in column V of Table 19.

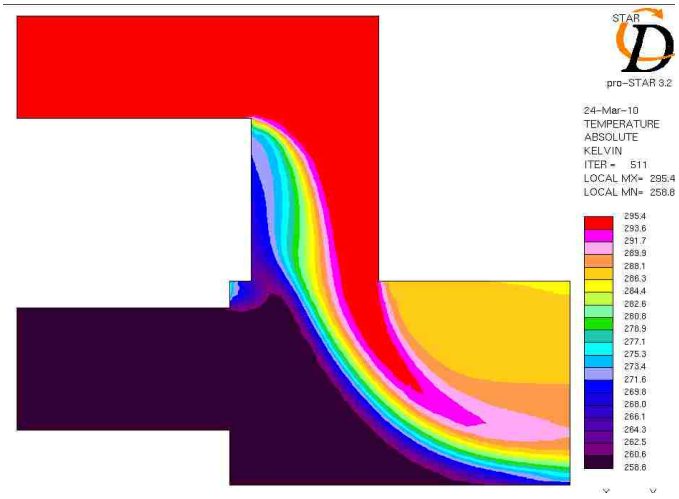

Figure 41. Temperature profile at section ABCDE with -15 °C of O.A

Figure 42 shows the velocity profile at the middle section (slice) of the mixing box with -15 ^{o}C outside air. Velocities from the experimental data are used for this simulation. Accuracy considerations are not

considered for this here. Turbulent eddies are formed in the mixing box due to local swirling motion.

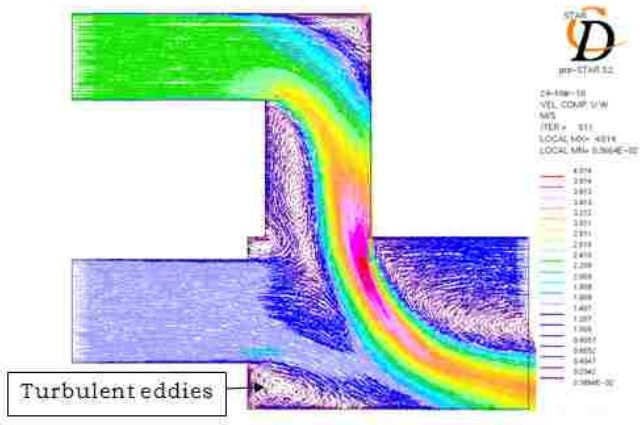

Figure 42. Velocity profile of section ABCDE with -15 °C of O.A

5.3.3 Experimental Uncertainty in Flow Rate and Temperature

Figure 43 shows the temperature profile at the middle section (slice) of mixing box with -5 ^{o}C outside air. In a more physically realistic situation, the experimental data reported by the velocity and temperature sensors are not so accurate. Some accuracy considerations have to be taken into account to make the simulations physically realistic. So this simulation is run by considering estimated uncertainties on both temperatures and velocities of return air and outside air. Accuracy consideration of + 0.8 K and - 0.6 K is taken on outside air temperature. Return air temperature is 295.4 K and outside air temperature is 268.8 K. The velocities of return air and outside air are 2.77 m/s and 1.36 m/s. Figure 44 shows

the velocity profile at the middle section plane ABCDE (slice) of the mixing box with -5 ºC outside air. The temperature difference between the upper and lower part of the duct is reported in column VI of Table 19.

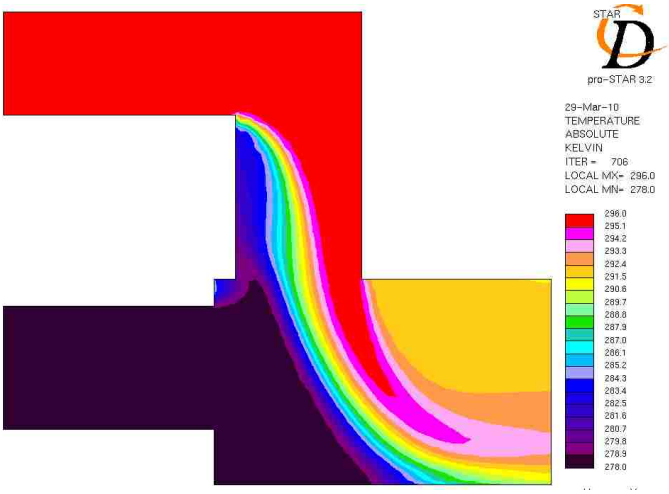

Figure 43. Temperature profile section ABCDE with -5 °C of O.A

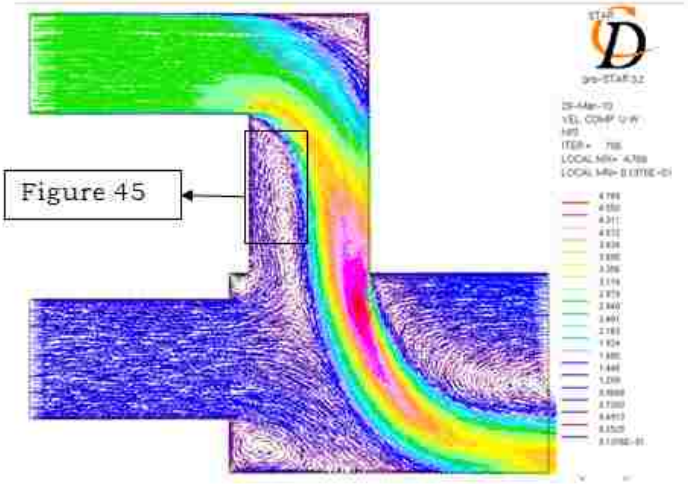

Figure 44. Velocity profile of section ABCDE with -5 °C of O.A

Figure 45 shows the profile of the recirculating zone in the mixing box. Recirculating zones are formed in the mixing box due to turbulence. Return air is supplied at a high velocity; as a result, negative pressure is created at the surface of the duct. This results in formation of a recirculating zone.

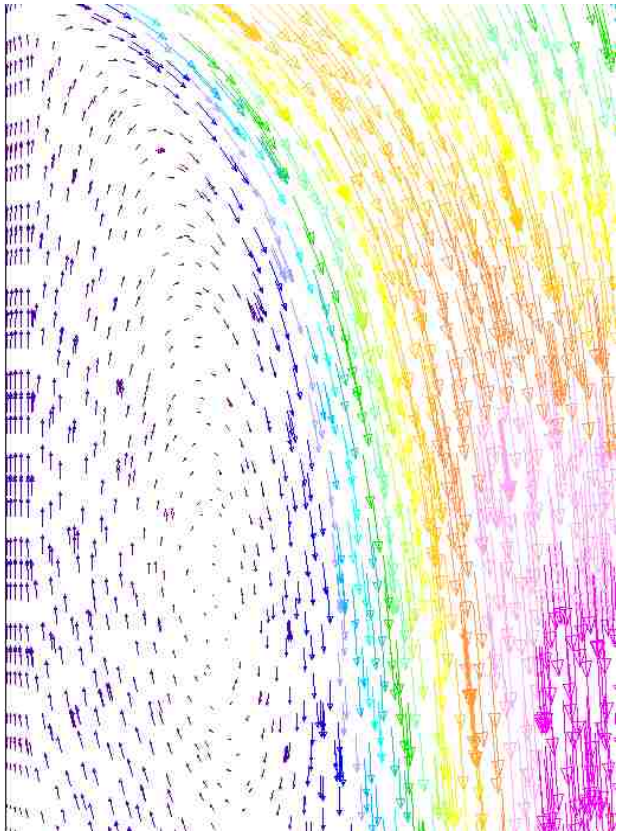

Figure 45. Recirculating zone formed in the mixing box

5.4 Simulations Run With Leakage

In a typical HVAC system, the mixing box is placed in the attic of the house or in larger installations in an unconditioned room. If leakage

exists on the suction side of the fan unit, the effect of leakage on the three variables in question: velocity, temperature and contaminant concentration need to be considered. To study this effect an artificial leakage of 1.5 ft × 0.041 ft is introduced on the suction side as shown in the Figure 46. Air is expected to enter the mixing box from the leakage site as it is a location of low pressure with respect to the ambient. Carbon dioxide and other pollutants will also enter the mixing box through the leakage as well. The temperature of air entering the mixing box from the leakage site is generally taken as the average of the return air temperature and outside air temperature. For the simulations involving leakage, the carbon dioxide concentration profile is plotted. The leakage is introduced into the mixing box with a velocity of 2 m/s.

The temperature distribution of the mixing box is shown in Figure 46. The outside air temperature is considered for this run to be 15 ^{o}C and the return air temperature is 23 ^{o}C. The temperature of air entering the mixing box from leakage is 277 K.

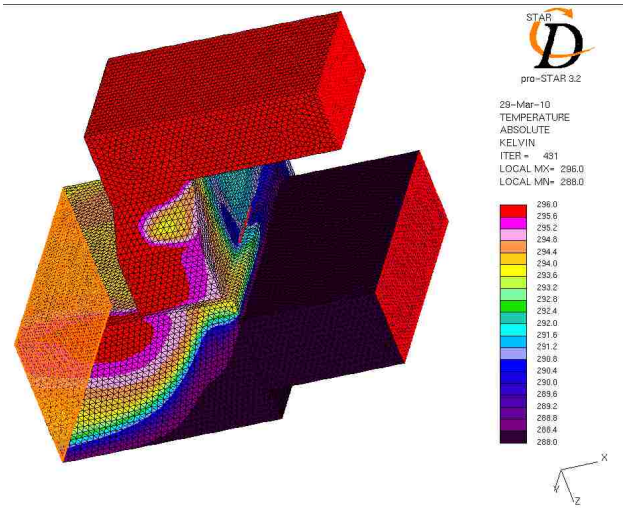

Figure 46. Temperature distribution with O.A at 15 °C

The carbon dioxide concentration of the outside air is maintained constant at 0.03%. Three different concentrations of the carbon dioxide are considered for the simulations. The carbon dioxide concentration of the return air is varied as shown below.

1) 0.04%

2) 0.06%

3) 0.08%

The temperature profile at the middle section plane ABCDE (slice) of mixing box at -15 ° C of outside air is shown in Figure 47. For all simulations involving leakage studies the experimental data for temperature and velocities of return air and outside air were used [23].

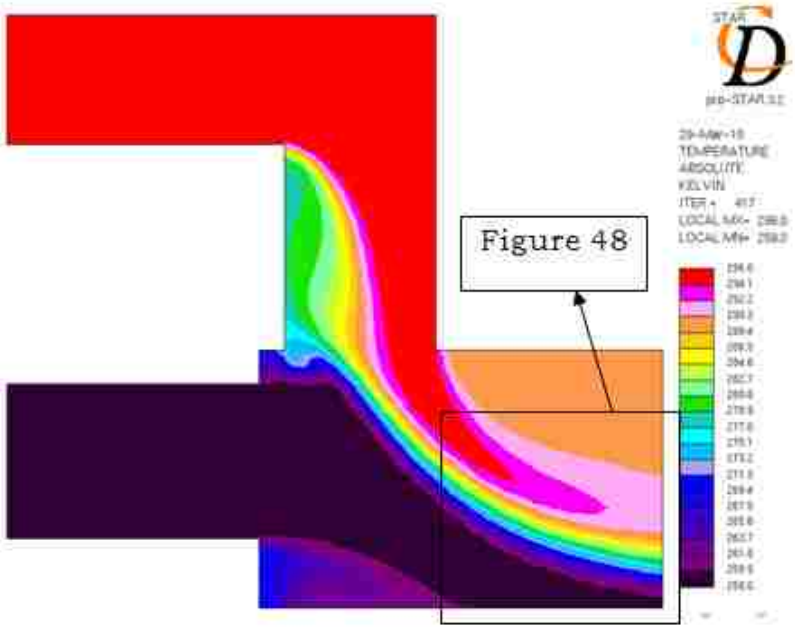

Figure 47. Temperature profile section ABCDE with -15 °C of O.A

Figure 48 shows the mixing effectiveness at the outlet of the mixing box decreases due to the effect of the leakage when compared to the simulations run with out considering leakage. The temperature difference between the upper and lower part of the mixing box increases. This can result in inaccurate temperature reading estimates at the outlet of the mixing box for potential control purposes and for thermal performance of the coil. The velocity profile at the middle section plane ABCDE (slice) of the mixing box at -15 ^{o}C of outside air is shown in Figure 49. The divergent angle of 180^{o} is noted at the intersection of the outside air duct and core of the mixing box. An increase in the cross sectional area of the

outside air duct causes a drop in the average flow velocity. This results in the formation of extensive zone of reverse recirculation.

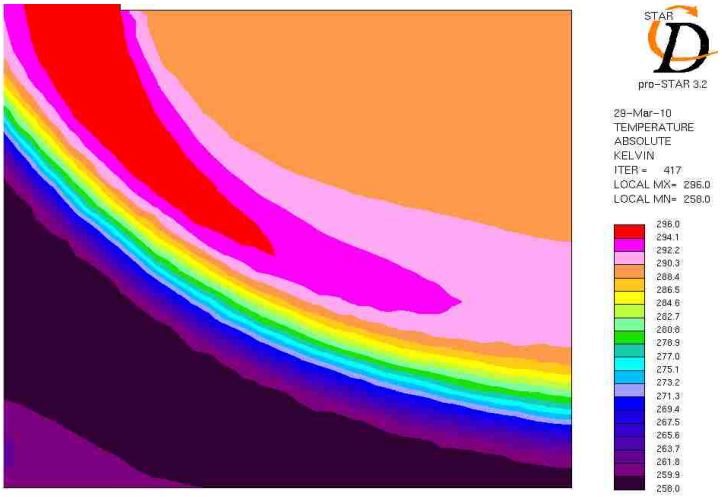

Figure 48. Temperature profile at the outlet of mixing box

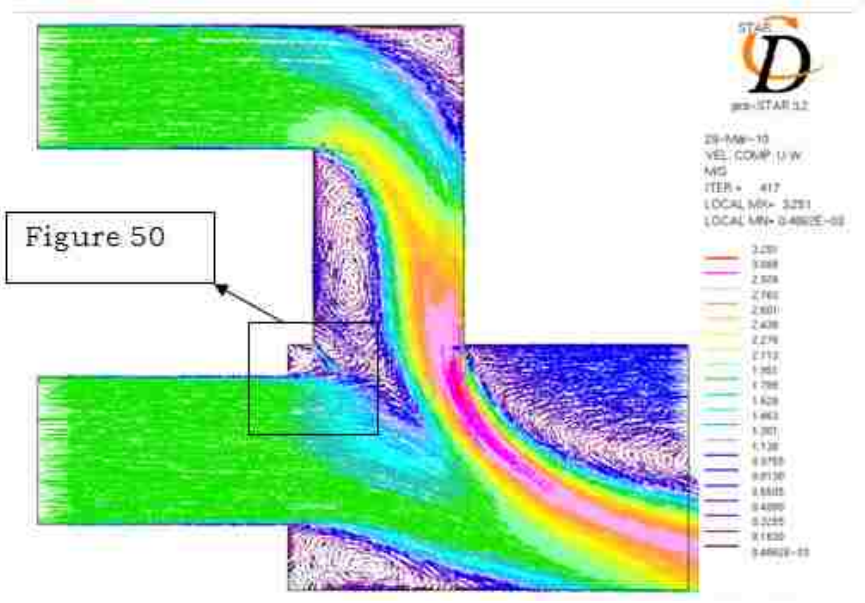

Figure 49. Velocity profile at section ABCDE with -15 °C of O.A

The effect of the leakage on the velocity profile is shown in Figure 50. Small eddies are formed due to the introduction of leakage into mixing box. Due to introduction of leakage, the number of recirculating zones is increased, thereby increasing the turbulence.

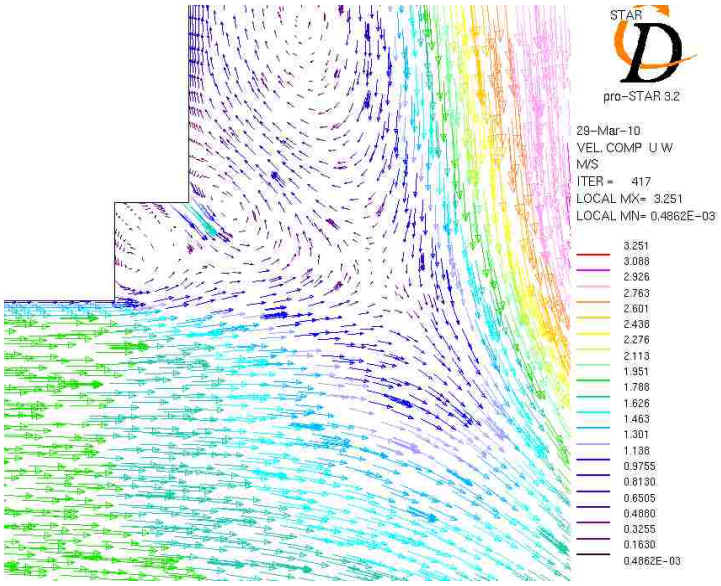

Figure 50. Velocity profile showing the effect of leakage

Carbon dioxide concentration profile at the middle section (slice) of the mixing box with -15 ^{o}C outside air is shown in Figure 51. Return air and outside air are supplied with a carbon dioxide concentration of 0.04 % and 0.03% respectively. Carbon dioxide concentration is not uniform at the recirculating zones. As the flow develops, carbon dioxide concentration diffuses across the outlet of the mixing box.

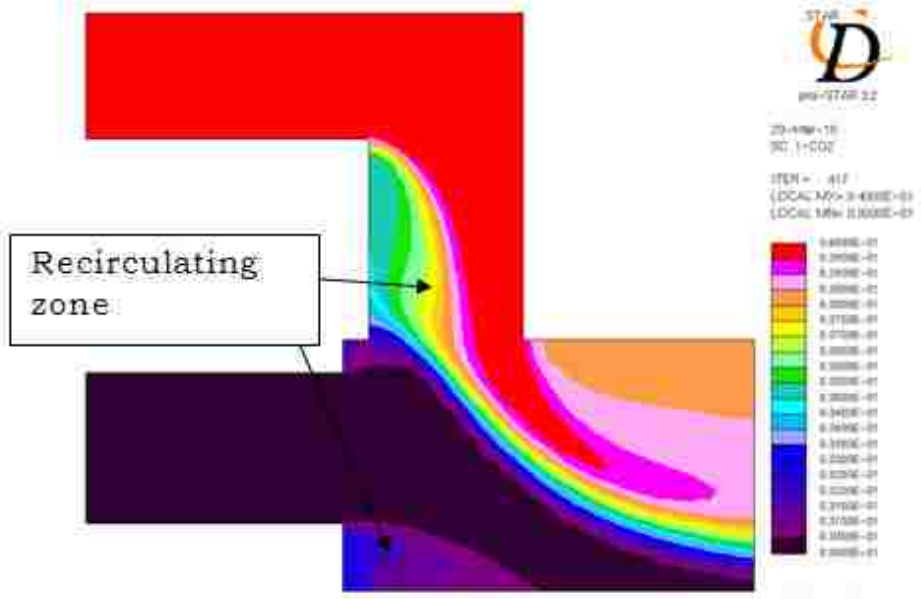

Figure 51. Carbon dioxide concentration profile at section ABCDE

The temperature profile at the middle section plane ABCDE (slice) of mixing box with 5 ^{o}C outside air is shown in Figure 52. The carbon dioxide concentration of the return air is 0.06%. The temperature of the air entering the mixing box from the leakage is assumed as the average temperature of the return air temperature and outside air temperature. The effect of leakage on the temperature profile of mixing box with 5 ^{o}C outside air is analyzed. Air enters the mixing box from the leakage at a temperature of 287K. The velocity of air entering from leakage is 2 m/s which is significantly higher than the return air (1.8m/s) and outside air (1.81m/s) velocities. This results in a little dip as shown in Figure 53.

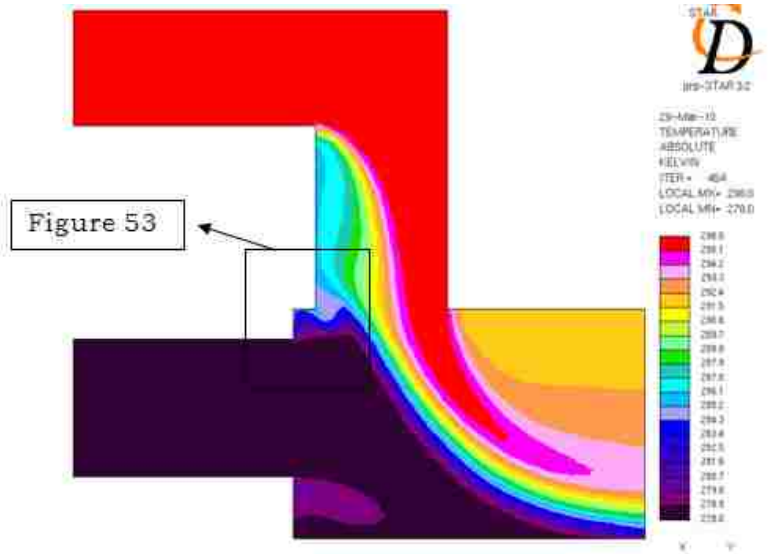

Figure 52. Temperature profile at section ABCDE with 5 °C of O.A

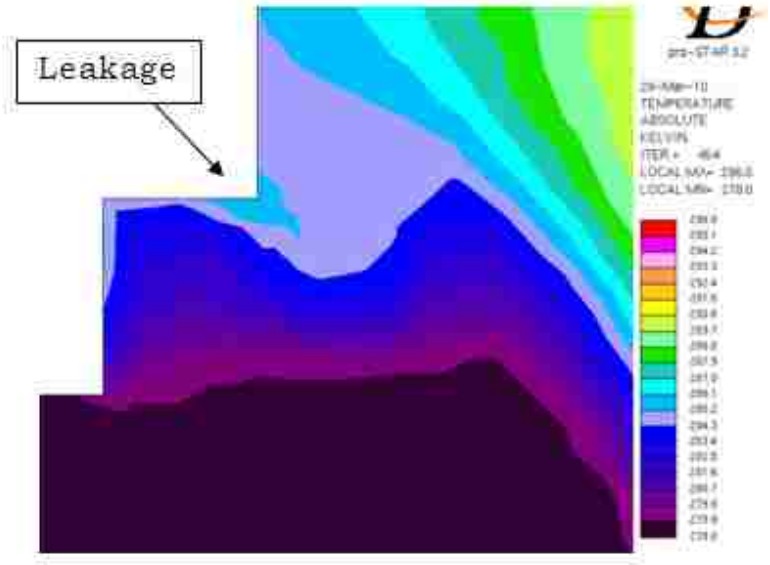

Figure 53. Effect of leakage on temperature profile with 5 °C of O.A

The temperature profile at the outlet duct of mixing box with 5 °C outside air is shown in Figure 54. The temperature difference between

the upper and lower part of the mixing box is considerable. The temperature distribution at the outlet of the duct is not uniform.

Figure 54. Temperature profile at the outlet duct with 5 °C of O.A

The velocity profile at the middle section plane ABCDE (slice) of the mixing box with 5 ^{o}C outside air is shown in Figure 55. Return air is supplied with a velocity of 2.12 m/s and outside air is supplied with a velocity of 1.58 m/s. The velocity of air entering the mixing box from leakage is 2 m/s. A significant drop in the velocity is noticed at the point where the outside air meets the air coming from the leakage.

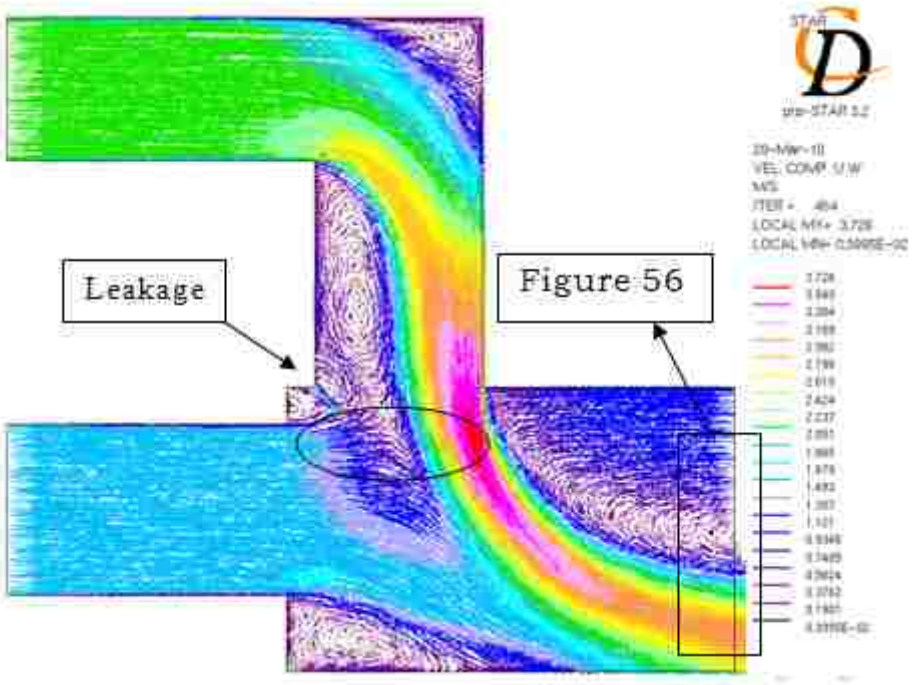

Figure 55. Velocity profile at section ABCDE with 5 °C of O.A

As shown in Figure 56, air is drawn back into the mixing box at the outlet duct. Because the mixed air velocity field does not get enough time to develop completely and being concentrated at the outlet of duct, it creates the conditions for flow reversal. So air flows back into mixing box in a reverse direction i.e. against the supply fan. The supply fan sucks the air from the outlet of the mixing box and supplies it to the heating/ cooling coil. Therefore, the load on the supply fan is increased due to certain deflection of air flow in the direction against the fan rotation.

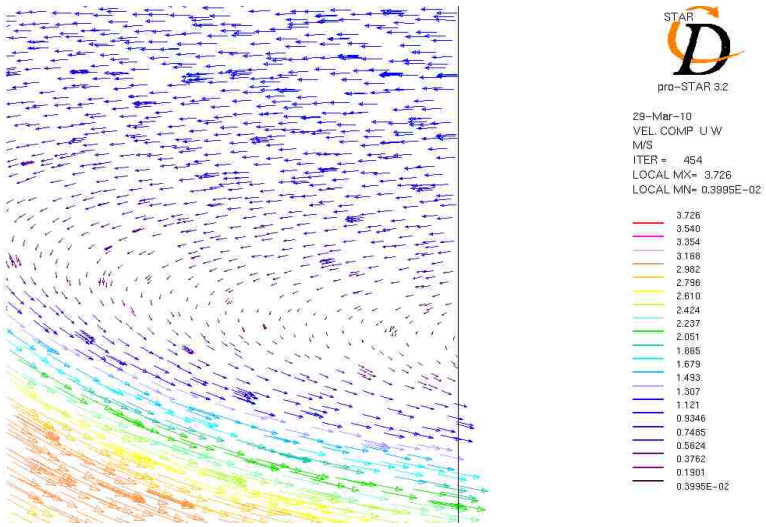

Figure 56. Air drawn back into the outlet duct of the mixing box

The carbon dioxide concentration profile at the middle section plane ABCDE (slice) of the mixing box with 5 ^{o}C outside air is shown in Figure 57. The carbon dioxide concentration of the return air is 0.06%. The carbon dioxide concentration of the outside air is 0.03%. Carbon dioxide entering the mixing box from the outside air duct diffuses into the small eddie that is formed due to the introduction of leakage as shown in Figure 58. Carbon dioxide entering the mixing box from the return air is evenly diffused and its concentration is decreased as it approaches the carbon dioxide entering the mixing box from leakage.

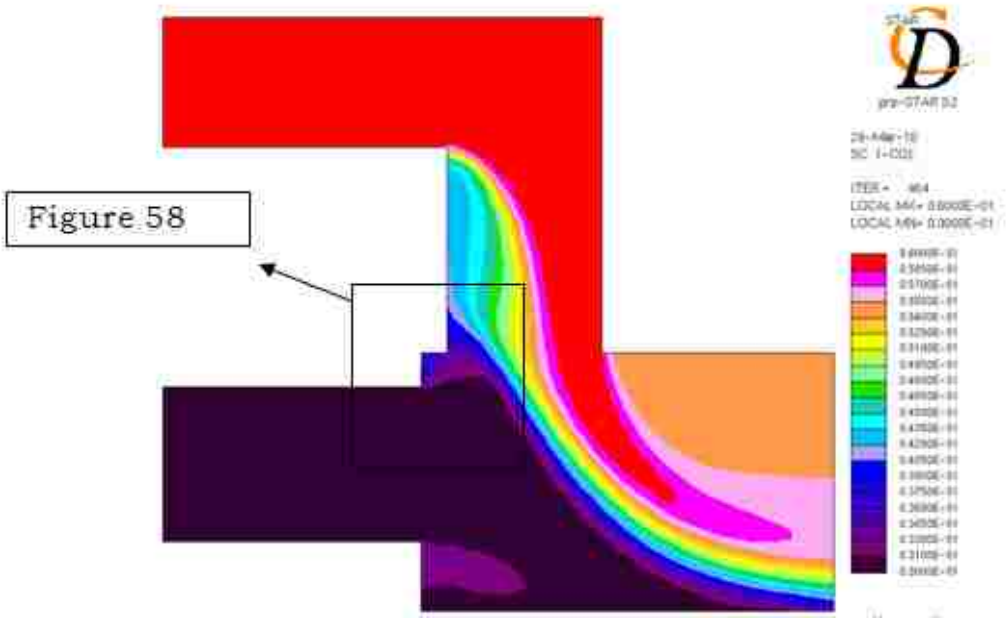

Figure 57. Carbon dioxide concentration profile at section ABCDE

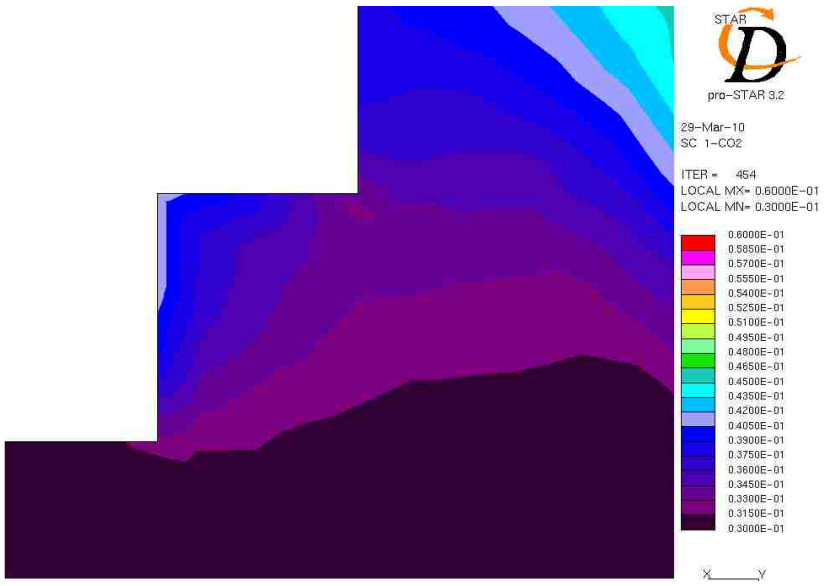

Figure 58. Effect of leakage on the carbon dioxide concentration

The experimental data by Par Carling [23] were obtained by using 8 sensors that were placed at the downstream (outlet) of the mixing box as shown in Figure 59.

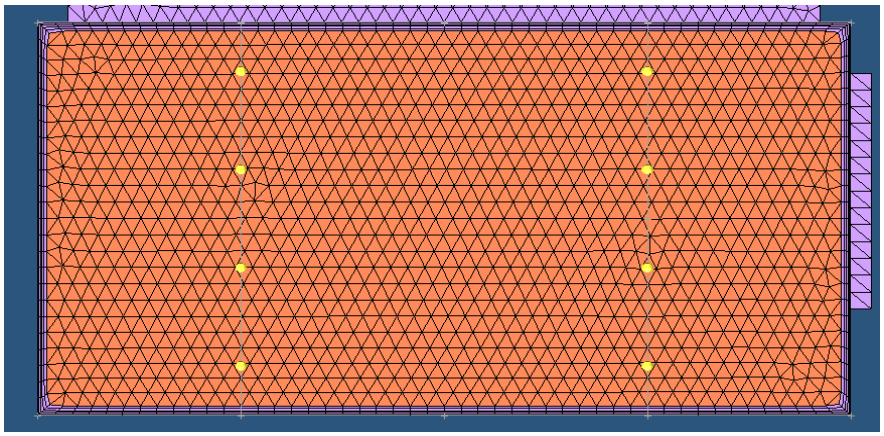

Figure 59.Sensors placed at the outlet as shown in the CFD grid

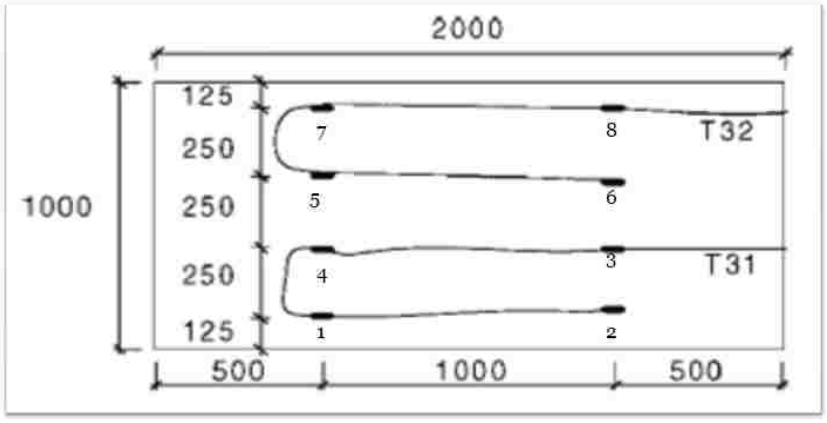

Figure 60. Cross section outlet of mixing box.

In Figure 60, 1, 2,3,4,5,6,7,8 are the sensors placed at the outlet of the mixing box. T 31 is the average temperature reported by sensors 1,2,3,4.

T 32 is the average temperature reported by sensors 5,6,7,8. All dimensions are in mm [23]

Table 19 shows the temperature difference between the T 32 and T31 [23]. As shown in the table there is considerably difference between the values obtained from the experimental data and the 2-D CFD simulations.

The values obtained from the 3-D simulations by considering the uncertainty in flow and temperature experimental data provided a better agreement with experimentally measured average flow and temperature. Par carling used a two-dimensional CFD model for simulations. A two-dimensional model does not give enough physical insight to predict stratification in a mixing box accurately [23]. So there were significant discrepancies between the experimental values and the 2-D simulated data. For obtaining better results and to make the model more physically realistic, a three-dimensional CFD model is used here for the simulations. The uncertainties reported by the sensors in the experimentally measured flow rates and temperatures are considered in order to create a realistic environment for the model. Further, the possibility of leakage and its effect on the temperature, velocity and carbon dioxide concentration is analyzed.

Table 19. Temperature difference between T 32 and T 31

Outside Air temperature (° C)	Temp. Difference from Experimental Data (Par Carling et al.2001) (° C)	Temp. Difference from 2D CFD simulations (Par Carling et al.2001) (° C)	Current 3D CFD Study using calculated temperature and velocities (° C)	Current 3D CFD Study using revised velocities (° C)	Current 3D CFD Study using revised temperatures & velocities (° C)
-15	6.2	17	19.07	9.96	9.8
-5	5	13	10.25	7.17	5
5	3	8	6.07	2.95	2.75
15	1.3	3.5	3.05	1	0.8

Increasing the length of the outlet duct will allow the flow to be fully developed. It provides a better opportunity for the air to be mixed. This allows a better estimate of the temperature for control purposes. Improved mixing allows a better prediction of the on-coil thermal conditions and hence can estimate that performance with more confidence.

Furthermore, a strong agreement between the temperature difference from experimental data and 3-D CFD study using revised temperatures and velocities is noted. This is achieved because the simulations are performed by simulating a physically realistic environment and providing more accurate boundary conditions.

Figure 61 shows the temperature difference between the upper and lower part of the mixing box at the outlet. It is noted that as the temperature of the outside air increases the difference in between the upper and lower part of the duct decreases. This phenomenon is as a result of decrease in the temperature difference in between the return air and outside air temperatures. As the temperature difference between the outside air and return air decreases better mixing is obtained. A uniform temperature distribution is noticed at the outlet of the duct. The temperature differences between the outside air and return air temperatures is decreased by taking accuracy considerations on both the return air and the outside air temperatures.

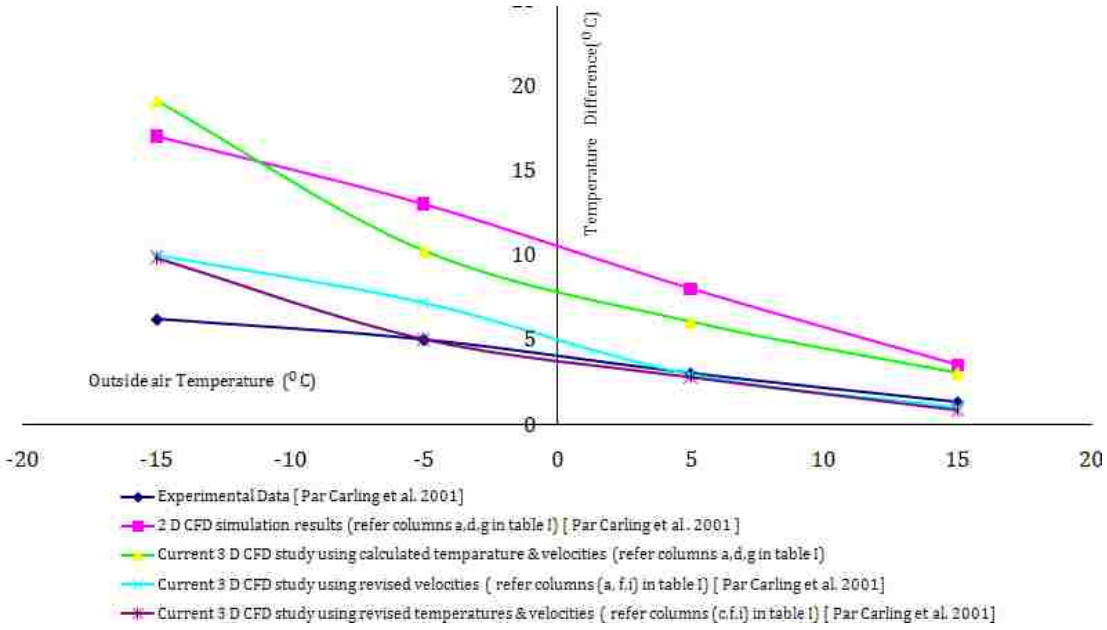

Figure 61. Temperature difference between T 32 and T 31

5.5 Discussion

Numerous designs of mixing boxes are available commercially. The mixing box tested in this paper was not designed according to the recommendations suggested by Haines [35]. Supplying cold air on top and warm air from the bottom results in better mixing [36].

Static air mixers can be used to improve mixing which enhance the mixing effectiveness, but at the cost of additional pressure loss. A static mixer is shown in Figure 62.

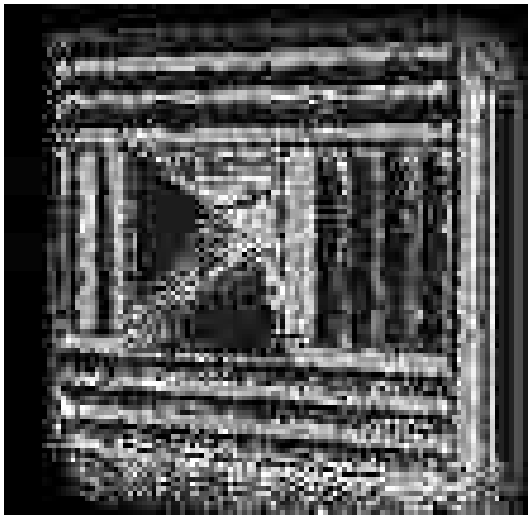

Figure 62. Static mixer used in air handling unit

They can be used to mix or blend outside and return air streams to a uniform temperature and velocity distribution. The air mixer thereby prevents temperature stratification, eliminates coil freeze-ups, and provides a uniform plenum velocity for equalized filter loading and

optimal coil performance [37]. Also space is a major constraint in design of air handling unit [38].

Moreover, as Stallborn's [36] measurements show, the air can be stratified in any direction further increasing the uncertainty. The use of the mixed air temperature for the purpose of control must therefore be questioned. Some fault detection and diagnosis methods for AHU's use the mixed air temperature as input. [23].

CHAPTER 6

CONCLUSIONS

6.1 Experimental Work

By using the proposed technique we can find both the total and local leakages effectively. By using this technique we can directly pin point the leaky locations (by finding the local leakage sites) and the duct sealing operation can be performed at the specific location instead of fixing whole house. The duct sealing is performed at the locations where high leaks are found. So this saves both time and money.

The proposed method is more cost effective when compared to other methods. It reduces the leakage rates for different houses by 2% to 11% of the total supply air flow. The method however as used in the field needs some improvement for its full implementation for residential use so that its full benefit can be realized. Part of the problem in some homes is that the “reachability” factor for the zone bag was compromised due to the fact that the plastic hose to which the bag was connected to perform the partial blockage tests could not be inserted deep enough to perform reasonable partial isolation of the different sections of the duct in some instances. Had this “reachability” factor been more enhanced a more detailed indicator for the intermediate leakage locations would have been made.

Some work is planned for an improved method based on this principle of the partial obstruction using a zone bag is intended with a national company who is interested in pursuing this matter and work with UNLV to develop the improved technology. It is felt though that using this improved method and standardized techniques of fixing leakages can be cost effective with other duct leakage/ repair techniques in the long run.

6.2. CFD Simulations

Four different outside air temperatures (-15 ° C, -5 ° C, 5 ° C, 15° C) and return air temperature of 23 ° C are used for the simulations. An artificial leakage of 1.5 ft × 0.041 ft is introduced at the suction side of the mixing box. Temperature, velocity and carbon dioxide profiles of a HVAC mixing box are studied using a CFD code.

The measurements and simulations presented here show that the temperature stratification downstream an AHU mixing box can be considerable. The sensors and their locations need to be chosen more judicially to accurately control the HVAC system as inaccurate readings can lead to coil freeze because of improper mixing as shown in the experiments/simulations.

Also this study shows that 3-D CFD modeling can accurately predict the important phenomena in regards to the function of the mixing box within the experimental uncertainty errors in the paper by Par

Carling [23]. Unfortunately the original study [23] did not give any localized temperature or velocity measurements in the box for more detailed comparisons.

This study also provides an insight about the carbon dioxide distribution in a mixing box. This helps in identifying an appropriate control system to adapt to $C0_2$ based ventilation control. This allows us to monitor the occupant comfort and satisfaction.

BIBLIOGRAPHY

[1]. Jump, D., I.S. Walker, and M.P. Modera. 1996. Field measurements of efficiency and duct retrofit effectiveness in residential forced air distribution systems. Proc. ACEEE Summer Study 1996, pp. 1.147-1.157.

[2]. Siegel, J., R. Davis, P. Francisco, et al. 1998. Measured heating system efficiency retrofits in eight manufactured (HUD Code) homes. Proc. ACEEE Summer Study1998, 2.189-2.201.

[3]. Cummings, J. B., J. J. Tooley, Jr., and R. Dunsmore. 1990. Impacts of Duct Leakage on Infiltration Rates, Space Conditioning Energy Use, and Peak Electrical Demand in Florida Homes. *Proceedings of ACEEE Summer Study, Pacific Grove, California,* August 1990. American Council for an Energy Efficient Economy, Washington, D.C.

[4]. Sherman, M., Walker, I., Dickerhoff, D. 2000. Stopping Duct Quacks: Longevity of Residential Duct Sealants. *Proceedings of ACEEE Summer Study*.

[5]. Francisco, P.W., L. Palmiter, and B. Davis. 2002a. Improved Ways to Measure Residential Duct Leakage. Final report for the American Society for Heating, Refrigerating, and Air-Conditioning Engineers. Report 1164-RP. Ecotope, Inc., Seattle, WA.

[6]. Francisco, P.W., L. Palmiter, and B. Davis. 2002b. “Field Performance of Two New Residential Duct Leakage Measurement Techniques”. Proceedings of the 2002 ACEEE Summer Study on Energy Efficiency in Buildings, Monterey, CA.

[7]. Francisco, P.W., L. Palmiter, and B. Davis. 2003. Insights into improved ways to measure residential duct leakage. ASHRAE Transactions 109(1) 485-740.

[8]. ASHRAE 2004. Method of Test for Determining the Design and Seasonal Efficiencies of Residential Thermal Distribution Systems. ANSI/ASHRAE 152-2004.

[9]. ASTM 2003. Standard Test Methods for Determining External Air Leakage of Air Distribution Systems by Fan Pressurization. E 1554 – 03.

[10]. Walker, I.S., M.H. Sherman, J. Wempen, D. Wang, and D.J. Dickerhoff. 2001. Development of a new duct leakage test: Delta Q. Lawrence Berkeley Laboratory, LBNL Report 47308.

[11]. Walker, I., M. Sherman, M. Modera and J. Siegel, 1998. Leakage Diagnostics, Sealant Longevity, Sizing and Technology Transfer in Residential Thermal Distribution Systems, Report submitted to Lawrence Berkeley National Laboratory, 1998.

[12]. Dickerhoff, D.J.; Sherman, M.H, and Walker, I.S.; 2004. Validating and Improving the Delta Q Duct Leakage Test. *ASHRAE Transactions* 110 (2): 741-751.

[13]. Francisco, P.W., and L. Palmiter. 2000. Field validation of Standard 152P. ASHRAE Transactions 106(2) 771-783.

[14]. Francisco, P.W., and L. Palmiter. 2001. The nulling test: A new measurement technique for estimating duct leakage in residential homes. ASHRAE Transactions 107(1) 297-303.

[15]. Francisco, P.W., L. Palmiter, E. Kruse, and B. Davis. 2004. Evaluation of two new duct leakage measurement methods in 51 homes. ASHRAE Transactions 110(2) 727-740.

[16]. Register film sealing by conservation strategies http://www.conservationstrategies.com/home/cs1/page_73_16/register_sealing_film.html, accessed on May 2, 2010.

[17]. Pressure pan by conservation strategies http://www.conservationstrategies.com/home/cs1/page_63_16/12x_14x_4__pressure_pan.html, accessed on May 2, 2010.

[18]. Moujaes, S. and N. Nassif. 2008. Duct Leakage Measurements in Residential Buildings. National Centre for Energy Management and Building Technologies, Task 5-11, Final Report NCEMBT-080215. Alexandria, Virginia: National Center for Energy Management and Building Technologies.

[19]. DP 1010
http://www.designpoly.com/tsb/dp1010tsb.pdf, accessed on May 5, 2010.

[20]. GE Window and Door Foam
http://www.geadvancedmaterials.com/geam/gesa/Residential/en/Products/ProductDetail/gesiliconeiwindowanddoor.html , accessed on May 5, 2010.

[21]. http://greatstuff.dow.com/greatstuff/diy/products/gc.htm , accessed on May 5, 2010.

[22]. Paragon Consulting Services, Measurement and Verification (M & V) Study, 2004. Air Conditioning Rebate Program 2004, Nevada Power, Las Vegas NV.

[23]. Par Carling and Yue Zou, 2001. A comparison of CFD-Simulations and measurements of temperature stratification in a mixing box of an air-handling unit, International Journal of Energy Research.

[24]. Fathi finaish, Hank Sauer and bob van becelaere.May 2002. Final report ASHRAE1045-TRP: Verifying mixed air damper and air mixing damper charecterstics.

[25]. Delaney TA, Maiocco TM, Vogel AG. 1984. Avoiding coil freeze up. Heating/Piping/Air Conditioning. December 83-85.

[26]. Carling P, Isakson P. 1999. Temperature measurement accuracy in an air-handling unit mixing box. Proceedings of the third International Symposium on HVAC Shenzhen, China, 922-928.

[27]. Yang CHY, Jiang Y. 1995. Sensor fault detection of HVAC system-system constraint and voting. Proceedings of the Pan Pacific Symposium on Building and urban Environmental Conditioning in Asia, Nagoya, Japan.

[28]. Wang SW, Wang JB. 1999. Law based sensor fault diagnosis and validation for building air-conditioning systems, International Journal of HVAC and R Research 5(4):353-380.

[29]. S.V.Patankar, Numerical Heat Transfer, Hemisphere, Washington 1980.

[30]. A.J.Baker, Finite element computational fluid mechanics, Hemisphere, Washington 1983.

[31]. STAR CD user manual, version 3.24. ADAPCO.

[32]. Pro/ENGINEER http://en.wikipedia.org/wiki/Pro/ENGINEER

[33]. Hand book of Hydraulic Resistance , second edition, revised and augmented, I.E.Idelchik,1986,Hemisphere Publishing Corporation.

[34]. Turbulence modeling for CFD, second edition, David C.Wilcox,1998 by DCW Industries,Inc.

[35]. Haines RW. 1980. Stratification. Heating/Piping/Air Conditioning. November 70-71.

[36]. Stallborn C. 1981. Blandningsproblem i ventilationsanlaggningar. Tekn. meddelanden 195. Inst. for Uppvarmnings- ochVentilationstek nik, KTH, Stockholm (in Swedish)

[37]. Static air mixer
http://www.kees.com/air_mixers.htm

[38]. Fathi finaish, Hank Sauer and bob van becelaere.May.2002.Final report ASHRAE1045-TRP: Verifying mixed air damper and air mixing damper characteristics.

VITA

Graduate College
University of Nevada, Las Vegas

Uday Vadlamani

Degrees:

Bachelor of Technology in Mechanical Engineering, 2007
Jawaharlal Nehru Technological University, India

Special Honors and Awards:

Recipient of ASHRAE Southern Nevada Student Grant for year 2008-2009

Thesis Title: Field Measurement & Verification of Residential Duct Leakage Methods and CFD Analysis of HVAC Mixing Box

Thesis Examination Committee:

Chairperson, Dr. Samir F. Moujaes Ph.D.
Committee Member, Dr. Robert F. Boehm, Ph.D.
Committee Member, Dr. Woosoon Yim, Ph.D
Graduate College Representative, Dr. Moses Karakouzian, Ph.D.